
from the many-body problem to DFT

the theory of nearly everything

$$\hat{H} = -\frac{1}{2} \sum_i \nabla_i^2 + \frac{1}{2} \sum_{i \neq i'} \frac{1}{|\mathbf{r}_i - \mathbf{r}_{i'}|} - \sum_{i, \alpha} \frac{Z_\alpha}{|\mathbf{r}_i - \mathbf{R}_\alpha|} - \sum_\alpha \frac{1}{2M_\alpha} \nabla_\alpha^2 + \frac{1}{2} \sum_{\alpha \neq \alpha'} \frac{Z_\alpha Z_{\alpha'}}{|\mathbf{R}_\alpha - \mathbf{R}_{\alpha'}|}$$

(atomic units: Appendix A)



Paul Adrien Maurice Dirac
Nobel Prize in Physics 1933

*The underlying laws needed for the description of all chemistry as well as a large part of physics are now entirely known. The only problem that remains is that the exact equations of quantum mechanics are too difficult to be solved. It is therefore necessary to derive **approximations** that allow us to calculate the properties of complex molecular systems with an acceptable computational effort.*

P.M.A. Dirac 1929

the many-body problem

$$\hat{H} = -\frac{1}{2} \sum_i \nabla_i^2 + \frac{1}{2} \sum_{i \neq i'} \frac{1}{|\mathbf{r}_i - \mathbf{r}_{i'}|} - \sum_{i,\alpha} \frac{Z_\alpha}{|\mathbf{r}_i - \mathbf{R}_\alpha|} - \sum_\alpha \frac{1}{2M_\alpha} \nabla_\alpha^2 + \frac{1}{2} \sum_{\alpha \neq \alpha'} \frac{Z_\alpha Z_{\alpha'}}{|\mathbf{R}_\alpha - \mathbf{R}_{\alpha'}|}$$

(atomic units: Appendix A)

Born-Oppenheimer Ansatz

$$\Psi(\{\mathbf{r}_i\}, \{\mathbf{R}_\alpha\}) = \psi(\{\mathbf{r}_i\}; \{\mathbf{R}_\alpha\}) \Phi(\{\mathbf{R}_\alpha\})$$

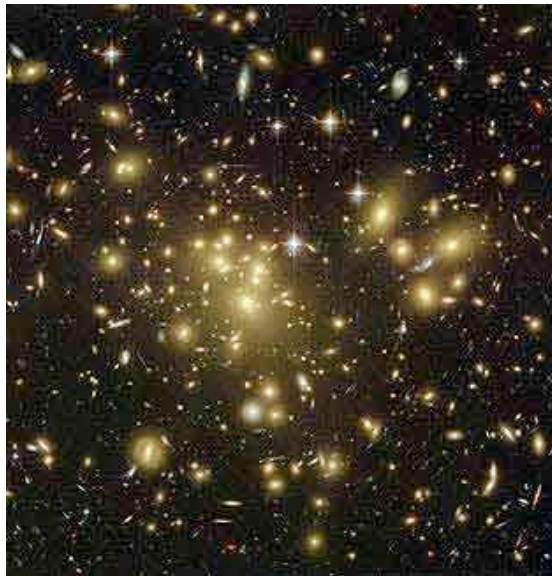
electronic Hamiltonian

$$\begin{aligned} \hat{H}_e &= -\frac{1}{2} \sum_i \nabla_i^2 + \frac{1}{2} \sum_{i \neq i'} \frac{1}{|\mathbf{r}_i - \mathbf{r}_{i'}|} - \sum_{i\alpha} \frac{Z_\alpha}{|\mathbf{r}_i - \mathbf{R}_\alpha|} + \frac{1}{2} \sum_{\alpha \neq \alpha'} \frac{Z_\alpha Z_{\alpha'}}{|\mathbf{R}_\alpha - \mathbf{R}_{\alpha'}|} \\ &= \hat{T}_e + \hat{V}_{ee} + \hat{V}_{en} + \hat{V}_{nn} \end{aligned}$$

a single iron atom



26 electrons, 78 arguments, 10^{78} values
10 X 10 X 10 grid



$$\Psi_0(\mathbf{r}_1, \mathbf{r}_1, \dots, \mathbf{r}_{26})$$

independent electrons

exact solution for $V_{ee}=0$

$$\hat{h}_e^0(\mathbf{r}) = -\frac{1}{2}\nabla^2 - \sum_{\alpha} \frac{Z_{\alpha}}{|\mathbf{r} - \mathbf{R}_{\alpha}|} = -\frac{1}{2}\nabla^2 + v_{\text{ext}}(\mathbf{r})$$

e.g. Bloch states, bands

many-body states

$$\psi(\{\mathbf{r}_i\}; \{\mathbf{R}_{\alpha}\}) = \frac{1}{\sqrt{N_e!}} \begin{vmatrix} \psi_{\mathbf{k}_1\uparrow}(\mathbf{r}_1) & \psi_{\mathbf{k}_1\uparrow}(\mathbf{r}_2) & \dots & \psi_{\mathbf{k}_1\uparrow}(\mathbf{r}_{N_e}) \\ \psi_{\mathbf{k}_1\downarrow}(\mathbf{r}_1) & \psi_{\mathbf{k}_1\downarrow}(\mathbf{r}_2) & \dots & \psi_{\mathbf{k}_1\downarrow}(\mathbf{r}_{N_e}) \\ \vdots & \vdots & \vdots & \vdots \\ \psi_{\mathbf{k}_{\frac{N_e}{2}}\uparrow}(\mathbf{r}_1) & \psi_{\mathbf{k}_{\frac{N_e}{2}}\uparrow}(\mathbf{r}_2) & \dots & \psi_{\mathbf{k}_{\frac{N_e}{2}}\uparrow}(\mathbf{r}_{N_e}) \\ \psi_{\mathbf{k}_{\frac{N_e}{2}}\downarrow}(\mathbf{r}_1) & \psi_{\mathbf{k}_{\frac{N_e}{2}}\downarrow}(\mathbf{r}_2) & \dots & \psi_{\mathbf{k}_{\frac{N_e}{2}}\downarrow}(\mathbf{r}_{N_e}) \end{vmatrix}$$

unfortunately Coulomb repulsion is large

density-functional theory

$$E[n] = F[n] + \int d\mathbf{r} v_{ext}(\mathbf{r})n(\mathbf{r}) + E_{nn} = F[n] + V[n] + E_{nn}$$

universal

$$n(\mathbf{r}) = n_0(\mathbf{r}) = \sum_n^{\text{occ}} |\psi_n(\mathbf{r})|^2$$

auxiliary independent electrons model

$$F[n] = T_0[n] + E_H[n] + E_{xc}[n] = T_0[n] + \frac{1}{2} \int d\mathbf{r} \int d\mathbf{r}' \frac{n(\mathbf{r})n(\mathbf{r}')}{|\mathbf{r} - \mathbf{r}'|} + E_{xc}[n]$$

Hartree Coulomb energy

long range and large

$$\hat{h}_e^0(\mathbf{r}) \psi_n(\mathbf{r}) = \left[-\frac{1}{2}\nabla^2 + v_R(\mathbf{r})\right]\psi_n(\mathbf{r}) = \varepsilon_n \psi_n(\mathbf{r})$$

Kohn-Sham equations

$$v_R(\mathbf{r}) = -\sum_{\alpha} \frac{Z_{\alpha}}{|\mathbf{r} - \mathbf{R}_{\alpha}|} + \int d\mathbf{r}' \frac{n(\mathbf{r}')}{|\mathbf{r} - \mathbf{r}'|} + \frac{\delta E_{xc}[n]}{\delta n}$$

exchange-correlation energy

$$E_{xc}[n] = E_{ee}[n] - E_H[n] + T_e[n] - T_0[n]$$

coupling-constant integration

$$V_{ee} \rightarrow \lambda V_{ee}$$

(see Lecture Notes, 6.3)

$$E_{xc}[n] = \int d\mathbf{r} \int d\mathbf{r}' \frac{n(\mathbf{r})n(\mathbf{r}')(\bar{g}(\mathbf{r}, \mathbf{r}') - 1)}{|\mathbf{r} - \mathbf{r}'|}$$

$$\bar{g}(\mathbf{r}, \mathbf{r}') = \int_0^1 d\lambda g_\lambda(\mathbf{r}, \mathbf{r}')$$

pair-correlation function

$$n(\mathbf{r}, \mathbf{r}') = \sum_{\sigma, \sigma'} n(\mathbf{r}\sigma, \mathbf{r}'\sigma') = n(\mathbf{r}')n(\mathbf{r})g_\lambda(\mathbf{r}, \mathbf{r}')$$

joint probability of finding electrons at \mathbf{r} and \mathbf{r}'

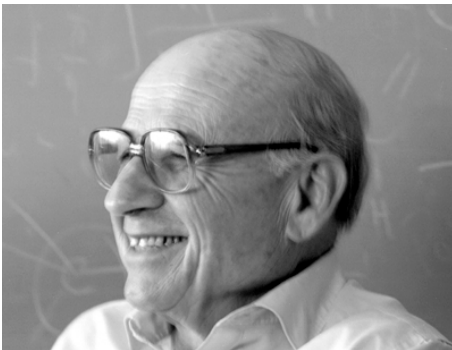
short-range and small

from DFT to LDA, GGA,...

$$E_{xc}[n] = \int d\mathbf{r} \int d\mathbf{r}' \frac{n(\mathbf{r})n(\mathbf{r}')(\bar{g}(\mathbf{r}, \mathbf{r}') - 1)}{|\mathbf{r} - \mathbf{r}'|}$$

$$E_{xc}[n] = \int d\mathbf{r} \epsilon_{xc}^{\text{LDA}}(n(\mathbf{r}))n(\mathbf{r})$$

homogeneous electron gas



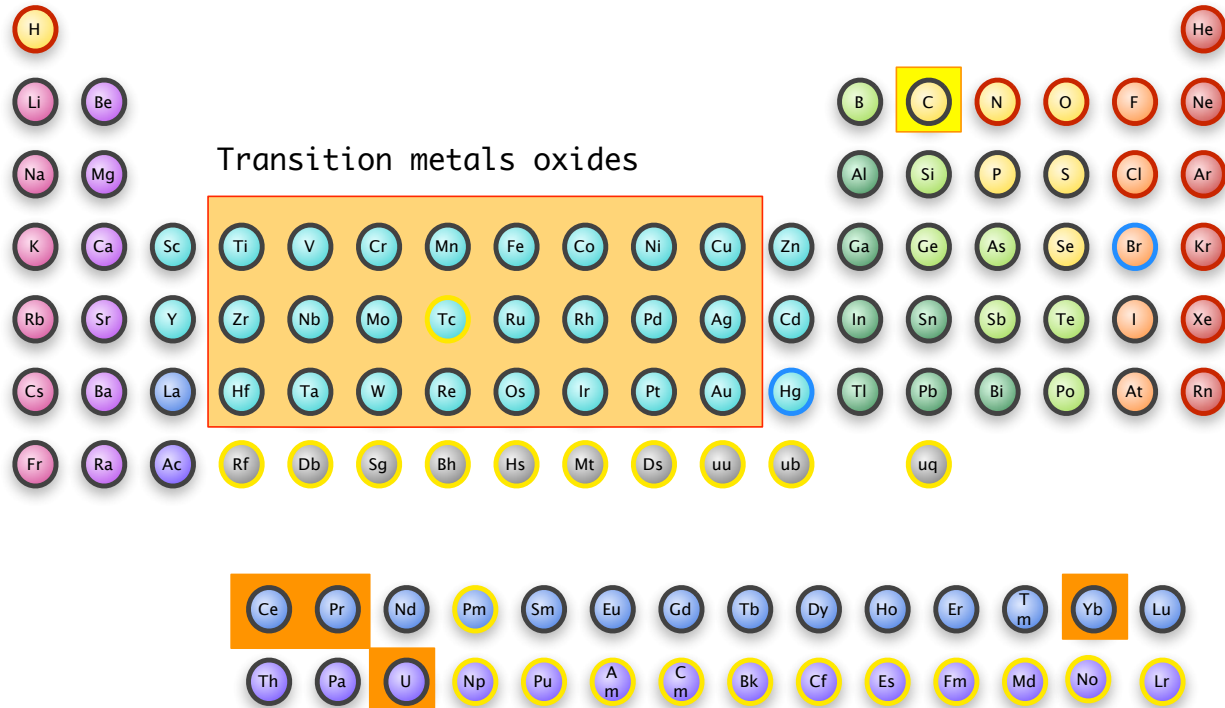
Walter Kohn

Nobel Prize in Chemistry (1998)

Kohn-Sham equations

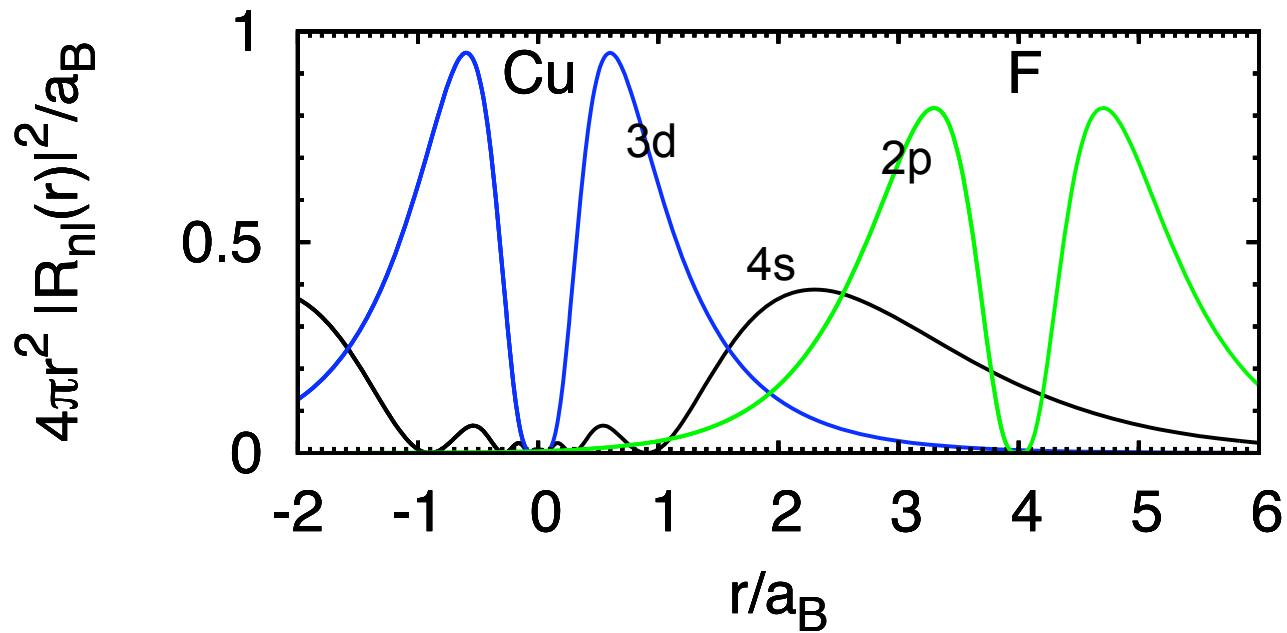
understand and predict properties
of solids, molecules, biological
systems, geological systems...

strongly correlated materials



example: Mott insulators metallic in LDA, GGA,..

localized electrons

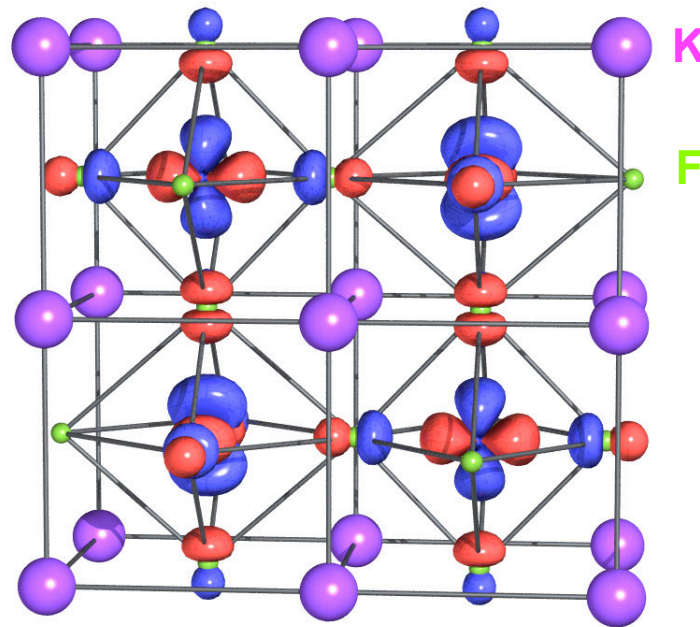


$$\psi_{nlm}(\rho, \theta, \phi) = R_{nl}(\rho) Y_l^m(\theta, \phi)$$

(hydrogen-like atom: Appendix B)

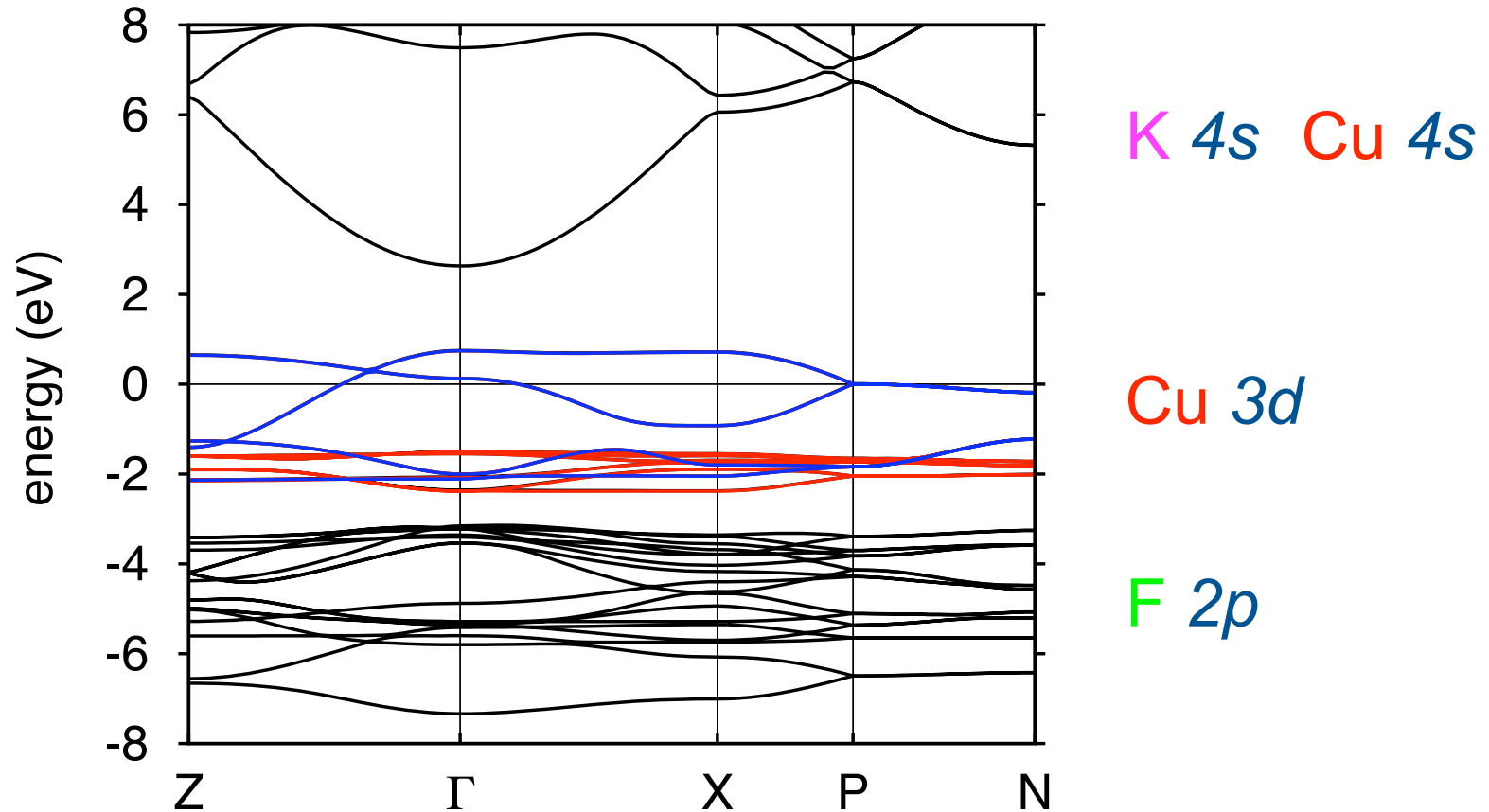
$$R_{nl}(\rho) = \sqrt{\left(\frac{2Z}{n}\right)^3 \frac{(n-l-1)!}{2n[(n+l)!]^3}} e^{-\rho/n} \left(\frac{2\rho}{n}\right)^l L_{n-l-1}^{2l+1}\left(\frac{2\rho}{n}\right)$$

an example: KCuF_3



odd number of electrons

LDA band structure



partially filled d-like bands, metallic

in reality: insulator, paramagnetic for $T > 40$ K

LDA, GGA, ...

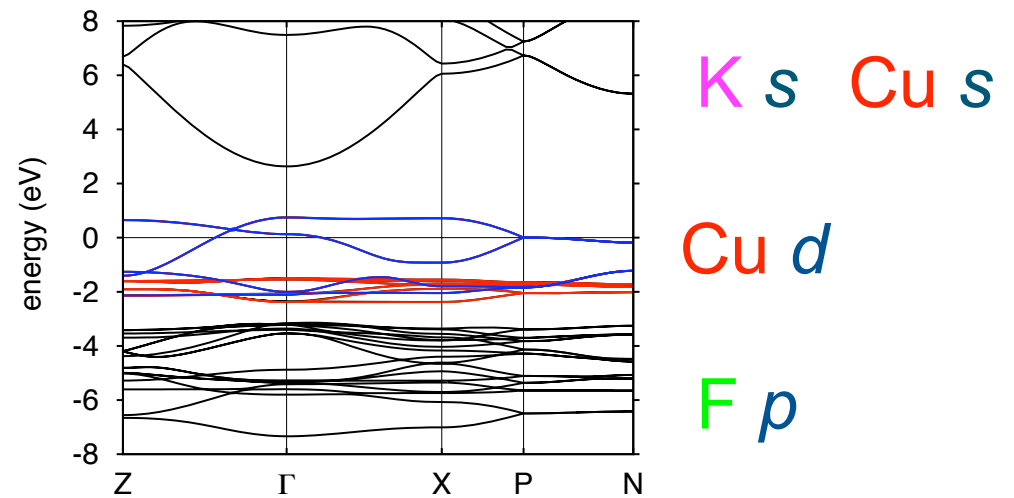
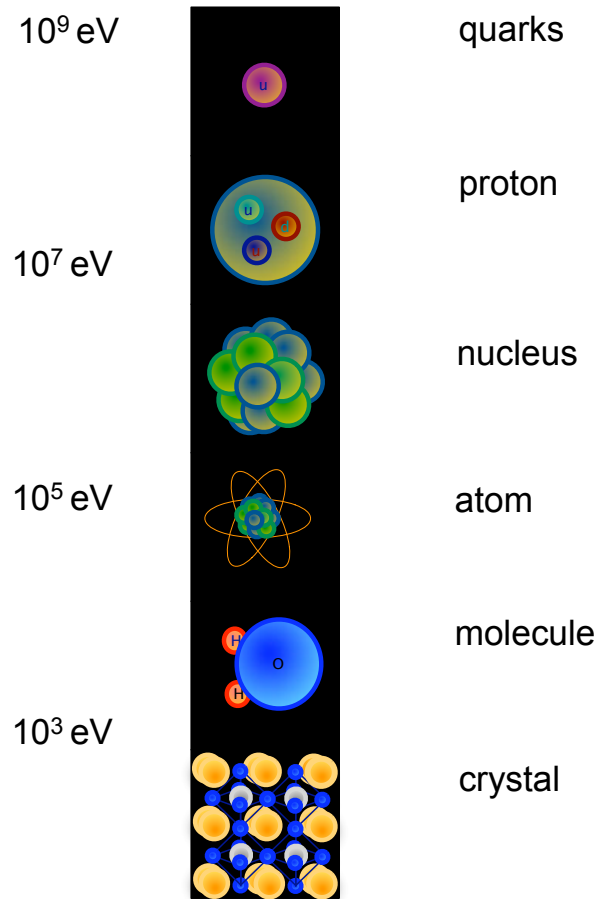
back to the many-body problem

$$\begin{aligned}\hat{H}_e &= -\frac{1}{2} \sum_i \nabla_i^2 + \frac{1}{2} \sum_{i \neq i'} \frac{1}{|\mathbf{r}_i - \mathbf{r}_{i'}|} - \sum_{i\alpha} \frac{Z_\alpha}{|\mathbf{r}_i - \mathbf{R}_\alpha|} + \frac{1}{2} \sum_{\alpha \neq \alpha'} \frac{Z_\alpha Z_{\alpha'}}{|\mathbf{R}_\alpha - \mathbf{R}_{\alpha'}|} \\ &= \hat{T}_e + \hat{V}_{ee} + \hat{V}_{en} + \hat{V}_{nn}\end{aligned}$$

simple models

from ab-initio to simple model

energy scales



simple low-energy models

simple models

real Hamiltonian

$$\begin{aligned}\hat{H}_e &= -\frac{1}{2} \sum_i \nabla_i^2 + \frac{1}{2} \sum_{i \neq i'} \frac{1}{|\mathbf{r}_i - \mathbf{r}_{i'}|} - \sum_{i\alpha} \frac{Z_\alpha}{|\mathbf{r}_i - \mathbf{R}_\alpha|} + \frac{1}{2} \sum_{\alpha \neq \alpha'} \frac{Z_\alpha Z_{\alpha'}}{|\mathbf{R}_\alpha - \mathbf{R}_{\alpha'}|} \\ &= \hat{T}_e + \hat{V}_{ee} + \hat{V}_{en} + \hat{V}_{nn}\end{aligned}$$

Hubbard model

$$\hat{H} = -t \sum_{\sigma \langle ii' \rangle} c_{i\sigma}^\dagger c_{i'\sigma} + U \sum_i \hat{n}_{i\uparrow} \hat{n}_{i\downarrow} = \hat{H}_0 + \hat{U}$$

$U=0$ half-filled band

$t=0$ isolated atoms

metal-insulator transition

dynamical mean-field theory

$$\hat{H} = -t \sum_{\sigma \langle ii' \rangle} c_{i\sigma}^\dagger c_{i'\sigma} + U \sum_i \hat{n}_{i\uparrow} \hat{n}_{i\downarrow} = \hat{H}_0 + \hat{U}$$

Hubbard model replaced by a
self-consistent one-impurity Anderson model

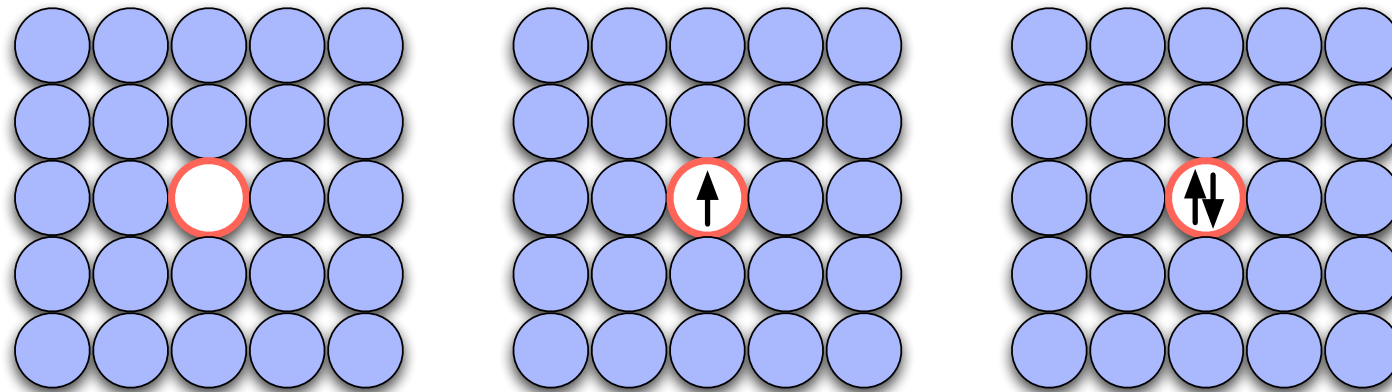
Anderson model

$$\hat{H}_{\text{eff}} = \sum_{\mathbf{k}\sigma} \varepsilon_{\mathbf{k}} \hat{n}_{\mathbf{k}\sigma} + \varepsilon_d \sum_{\sigma} \hat{n}_{d\sigma} + U \hat{n}_{d\uparrow} \hat{n}_{d\downarrow} + \sum_{\mathbf{k}\sigma} (V_{\mathbf{k}d} c_{\mathbf{k}\sigma}^\dagger d_{\sigma} + \bar{V}_{\mathbf{k}d} d_{\sigma}^\dagger c_{\mathbf{k}\sigma})$$

self-consistent parameters

solution: Bethe Ansatz NRG ED/Lanczos QMC

dynamical mean-field theory

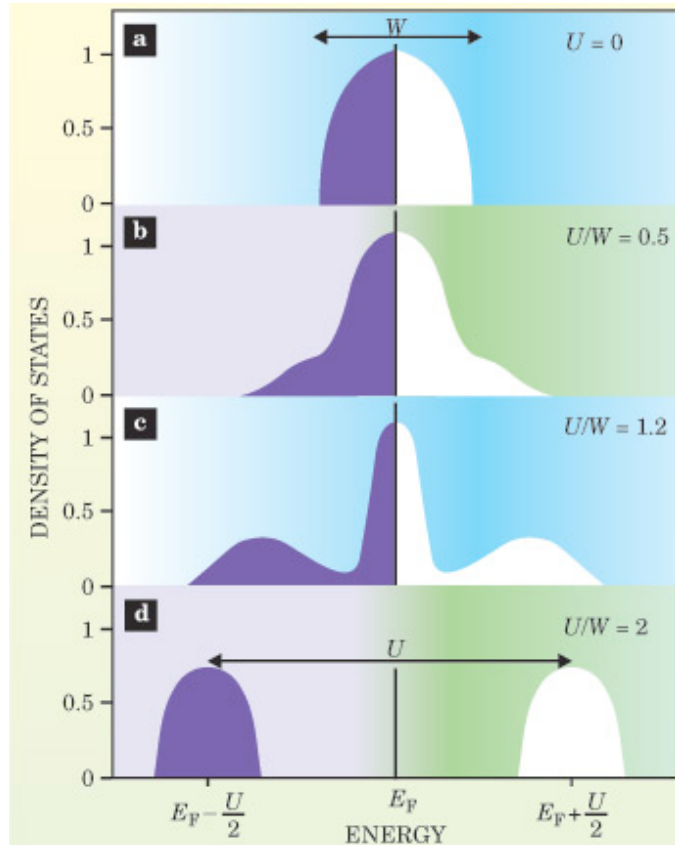


$$G_0^{-1} - G^{-1} = \Sigma(\omega)$$

dynamics captured self-energy local
exact in infinite dimensions

metal-insulator transition

Bethe lattice



G. Koltiar and D. Vollhardt
Physics Today **57**, 53 (2004)

metallic phase

$$\text{Re}\Sigma(\omega + i0^+) = U/2 + (1 - 1/Z)\omega + O(\omega^3), \quad (226)$$

$$\text{Im}\Sigma(\omega + i0^+) = -B\omega^2 + O(\omega^4). \quad (227)$$

The quasiparticle residue Z defines the renormalized Fermi energy of the problem:

$$\epsilon_F^* \equiv ZD \quad (228)$$

This is also the Kondo temperature of the impurity model. Since the self-energy is momentum independent, Z directly yields the effective mass of quasiparticles (Müller-Hartmann, 1989c):

$$\frac{m^*}{m} = \frac{1}{Z} = 1 - \frac{\partial}{\partial \omega} \text{Re}\Sigma(\omega + i0^+) \Big|_{\omega=0}. \quad (229)$$

insulating phase

$$\text{Im}\Sigma(\omega + i0^+) = -\pi\rho_2\delta(\omega) \quad \text{for } \omega \in [-\Delta_g/2, \Delta_g/2] \quad (235)$$

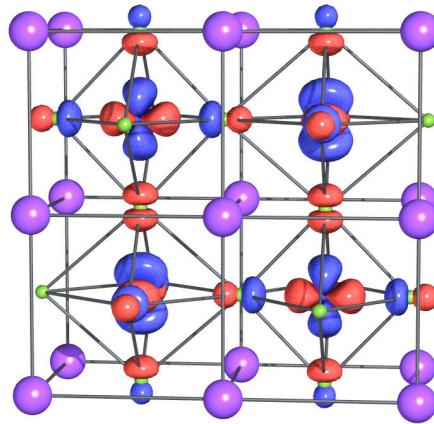
and that $\text{Re}\Sigma$ has the following low-frequency behavior:

$$\text{Re}\Sigma(\omega + i0^+) - U/2 = \frac{\rho_2}{\omega} + O(\omega). \quad (236)$$

A. Georges et al. RMP **63**, 13 (1996)

and real materials?

$$\hat{H} = -t \sum_{\sigma \langle ii' \rangle} c_{i\sigma}^\dagger c_{i'\sigma} + U \sum_i \hat{n}_{i\uparrow} \hat{n}_{i\downarrow} = \hat{H}_0 + \hat{U}$$



many bands
U tensor
crystal-field
non-local U
.....

$$\begin{aligned} \hat{H}_e &= -\frac{1}{2} \sum_i \nabla_i^2 + \frac{1}{2} \sum_{i \neq i'} \frac{1}{|\mathbf{r}_i - \mathbf{r}_{i'}|} - \sum_{i\alpha} \frac{Z_\alpha}{|\mathbf{r}_i - \mathbf{R}_\alpha|} + \frac{1}{2} \sum_{\alpha \neq \alpha'} \frac{Z_\alpha Z_{\alpha'}}{|\mathbf{R}_\alpha - \mathbf{R}_{\alpha'}|} \\ &= \hat{T}_e + \hat{V}_{ee} + \hat{V}_{en} + \hat{V}_{nn} \end{aligned}$$

increasing number of free parameters, difficult to test theory

from DFT to many-body models

realistic models

basis functions

$$\psi_{in\sigma}(\mathbf{r}) = \frac{1}{\sqrt{N}} \sum_{\mathbf{k}} e^{-i\mathbf{R}_i \cdot \mathbf{k}} \psi_{n\mathbf{k}\sigma}(\mathbf{r}) \quad \text{localized Wannier functions from LDA (GGA,...)}$$

Hamiltonian

$$\hat{H}_e = \hat{H}^{\text{LDA}} + \hat{U} - \hat{H}_{\text{DC}}$$

$$\hat{H}^{\text{LDA}} = - \sum_{\sigma} \sum_{in,i'n'} t_{n,n'}^{i,i'} c_{in\sigma}^{\dagger} c_{i'n'\sigma}$$

LDA Hamiltonian

$$t_{n,n'}^{i,i'} = - \int d\mathbf{r} \bar{\psi}_{in\sigma}(\mathbf{r}) \left[-\frac{1}{2} \nabla^2 + v_{\text{R}}(r) \right] \psi_{i'n'\sigma}(\mathbf{r})$$

Coulomb and double counting

$$\hat{U} = \frac{1}{2} \sum_{ii'jj'} \sum_{\sigma\sigma'} \sum_{nn'pp'} U_{np\ n'p'}^{iji'j'} c_{in\sigma}^\dagger c_{jp\sigma'}^\dagger c_{j'p'\sigma'} c_{i'n'\sigma}$$

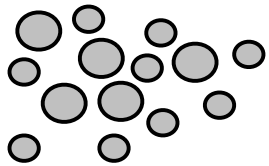
$$\begin{aligned} \hat{U} &= \frac{1}{2} U_{np\ n'p'}^{iji'j'} = \langle in\sigma\ jp\sigma' | \hat{U} | i'n'\sigma\ j'p'\sigma' \rangle \\ &= \int d\mathbf{r}_1 \int d\mathbf{r}_2 \bar{\psi}_{in\sigma}(\mathbf{r}_1) \bar{\psi}_{jp\sigma'}(\mathbf{r}_2) \frac{1}{|\mathbf{r}_1 - \mathbf{r}_2|} \psi_{j'p'\sigma'}(\mathbf{r}_2) \psi_{i'n'\sigma}(\mathbf{r}_1) \end{aligned}$$

\hat{H}_{DC} long range Hartree and mean-field exchange-correlation
already are well described by LDA (GGA,...)

up to here all electrons are the same....

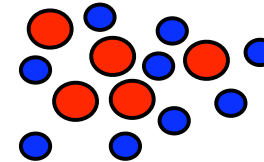
light and heavy electrons

electrons



light (weakly correlated): LDA (GGA,...)

heavy (strongly correlated): U



$$\hat{H}_e = \hat{H}^{\text{LDA}} + \hat{U}^l - \hat{H}_{\text{DC}}^l$$

eg. / shell

$$\hat{U}^l - \hat{H}_{\text{DC}}^l$$

short-range correction to LDA

local or almost local

for a / shell, the local Coulomb interaction is

$$\hat{U}^l = \frac{1}{2} \sum_i \sum_{\sigma\sigma'} \sum_{m_\alpha m'_\alpha} \sum_{m_\beta m'_\beta} U_{m_\alpha m_\beta m'_\alpha m'_\beta} c_{im_\alpha\sigma}^\dagger c_{im_\beta\sigma'}^\dagger c_{im'_\beta\sigma'} c_{im'_\alpha\sigma}$$

screening? cRPA, cLDA

Coulomb interaction tensor

$$\frac{1}{|\mathbf{r}_1 - \mathbf{r}_2|} = \sum_{k=0}^{\infty} \frac{r_{<}^k}{r_{>}^{k+1}} \frac{4\pi}{2k+1} \sum_{q=-k}^k Y_q^k(\theta_2, \phi_2) \bar{Y}_q^k(\theta_1, \phi_1)$$

$$U_{m_\alpha m_\beta m'_\alpha m'_\beta} = \sum_{k=0}^{2l} a_k(m_\alpha m'_\alpha, m_\beta m'_\beta) F_k \quad \text{d electrons: } F_0, F_2, F_4$$

$$a_k(m_\alpha m'_\alpha, m_\beta m'_\beta) = \frac{4\pi}{2k+1} \sum_{q=-k}^k \langle l m_\alpha | Y_q^k | l m'_\alpha \rangle \langle l m_\beta | \bar{Y}_q^k | l m'_\beta \rangle \quad \text{radial integral}$$

$$F_k = \int dr_1 r_1^2 \int dr_2 r_2^2 R_{nl}^2(r_1) \frac{r_{<}^k}{r_{>}^{k+1}} R_{nl}^2(r_2). \quad \text{Slater integral}$$

Coulomb interaction tensor

two-index terms

$$U_{mm'mm'} = U_{m,m'} = \sum_{k=0}^{2l} a_k(mm, m'm')F_k,$$
$$U_{mm'm'm} = J_{m,m'} = \sum_{k=0}^{2l} a_k(mm', m'm)F_k$$

direct and exchange integrals

$$U_{m,m'} = \int d\mathbf{r}_1 \int d\mathbf{r}_2 \bar{\psi}_{m\sigma}(\mathbf{r}_1) \bar{\psi}_{m'\sigma'}(\mathbf{r}_2) \frac{1}{|\mathbf{r}_1 - \mathbf{r}_2|} \psi_{m'\sigma'}(\mathbf{r}_2) \psi_{m\sigma}(\mathbf{r}_1)$$
$$J_{m,m'} = \int d\mathbf{r}_1 \int d\mathbf{r}_2 \bar{\psi}_{m\sigma}(\mathbf{r}_1) \bar{\psi}_{m'\sigma}(\mathbf{r}_2) \frac{1}{|\mathbf{r}_1 - \mathbf{r}_2|} \psi_{m\sigma}(\mathbf{r}_2) \psi_{m'\sigma}(\mathbf{r}_1)$$

density-density approximation

$$\hat{U}^l \sim \frac{1}{2} \sum_{i\sigma} \sum_{mm'} U_{m,m'} \hat{n}_{im\sigma} \hat{n}_{im'-\sigma} + \frac{1}{2} \sum_{i\sigma} \sum_{m \neq m'} (U_{m,m'} - J_{m,m'}) \hat{n}_{im\sigma} \hat{n}_{im'\sigma}$$

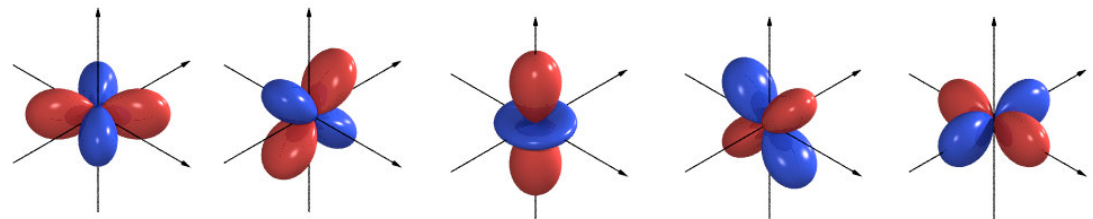
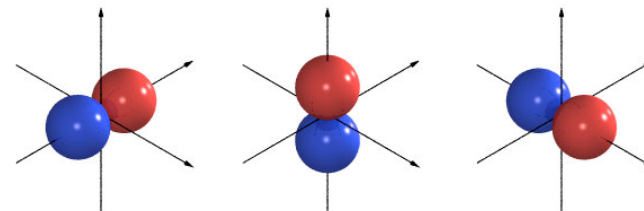
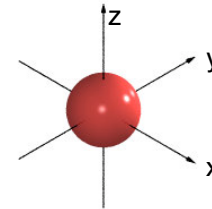
real harmonics

$$s = y_{00} = Y_0^0 = \sqrt{\frac{1}{4\pi}}$$

$$p_y = y_{1-1} = \frac{i}{\sqrt{2}}(Y_1^1 + Y_{-1}^1) = \sqrt{\frac{3}{4\pi}} \quad y/r$$

$$p_z = y_{10} = Y_1^0 = \sqrt{\frac{3}{4\pi}} \quad z/r$$

$$p_x = y_{11} = \frac{1}{\sqrt{2}}(Y_1^1 - Y_{-1}^1) = \sqrt{\frac{3}{4\pi}} \quad x/r$$



$$d_{xy} = y_{2-2} = \frac{i}{\sqrt{2}}(Y_2^2 - Y_{-2}^2) = \sqrt{\frac{15}{4\pi}} \quad xy/r^2$$

$$d_{yz} = y_{2-1} = \frac{i}{\sqrt{2}}(Y_1^2 + Y_{-1}^2) = \sqrt{\frac{15}{4\pi}} \quad yz/r^2$$

$$d_{3z^2-r^2} = y_{20} = Y_2^0 = \sqrt{\frac{15}{4\pi}} \frac{1}{2\sqrt{3}} (3z^2 - r^2)/r^2$$

$$d_{xz} = y_{21} = \frac{1}{\sqrt{2}}(Y_1^2 - Y_{-1}^2) = \sqrt{\frac{15}{4\pi}} \quad xz/r^2$$

$$d_{x^2-y^2} = y_{22} = \frac{1}{\sqrt{2}}(Y_2^2 + Y_{-2}^2) = \sqrt{\frac{15}{4\pi}} \frac{1}{2} (x^2 - y^2)/r^2$$

Coulomb tensor d shell

$U_{m,m'}^l$	$ xy\rangle$	$ yz\rangle$	$ 3z^2 - r^2\rangle$	$ xz\rangle$	$ x^2 - y^2\rangle$
$ xy\rangle$	U_0	$U_0 - 2J_1$	$U_0 - 2J_2$	$U_0 - 2J_1$	$U_0 - 2J_3$
$ yz\rangle$	$U_0 - 2J_1$	U_0	$U_0 - 2J_4$	$U_0 - 2J_1$	$U_0 - 2J_1$
$ 3z^2 - r^2\rangle$	$U_0 - 2J_2$	$U_0 - 2J_4$	U_0	$U_0 - 2J_4$	$U_0 - 2J_2$
$ xz\rangle$	$U_0 - 2J_1$	$U_0 - 2J_1$	$U_0 - 2J_4$	U_0	$U_0 - 2J_1$
$ x^2 - y^2\rangle$	$U_0 - 2J_3$	$U_0 - 2J_1$	$U_0 - 2J_2$	$U_0 - 2J_1$	U_0

$$U_{avg} = \frac{1}{(2l+1)^2} \sum_{m,m'} U_{m,m'} = F_0$$

$$U_{avg} - J_{avg} = \frac{1}{2l(2l+1)} \sum_{m,m'} (U_{m,m'} - J_{m,m'})$$

$$J_{avg} = (F_2 + F_4)/14$$

$$U_0 = U_{avg} + \frac{8}{7} J_{avg} = U_{avg} + \frac{8}{5} \mathcal{J}_{avg}$$

$$J_1 = \frac{3}{49} F_2 + \frac{20}{9} \frac{1}{49} F_4$$

$$J_2 = -2\mathcal{J}_{avg} + 3J_1$$

$$J_3 = 6\mathcal{J}_{avg} - 5J_1$$

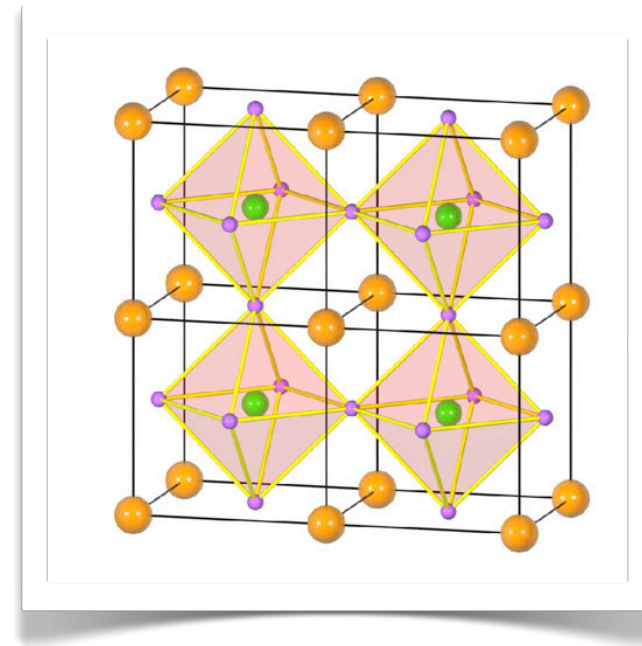
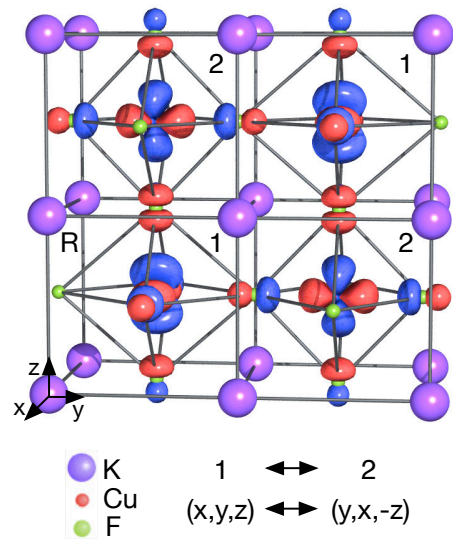
$$J_4 = 4\mathcal{J}_{avg} - 3J_1$$

atomic $3d$ $F_4/F_2 = 15/23$

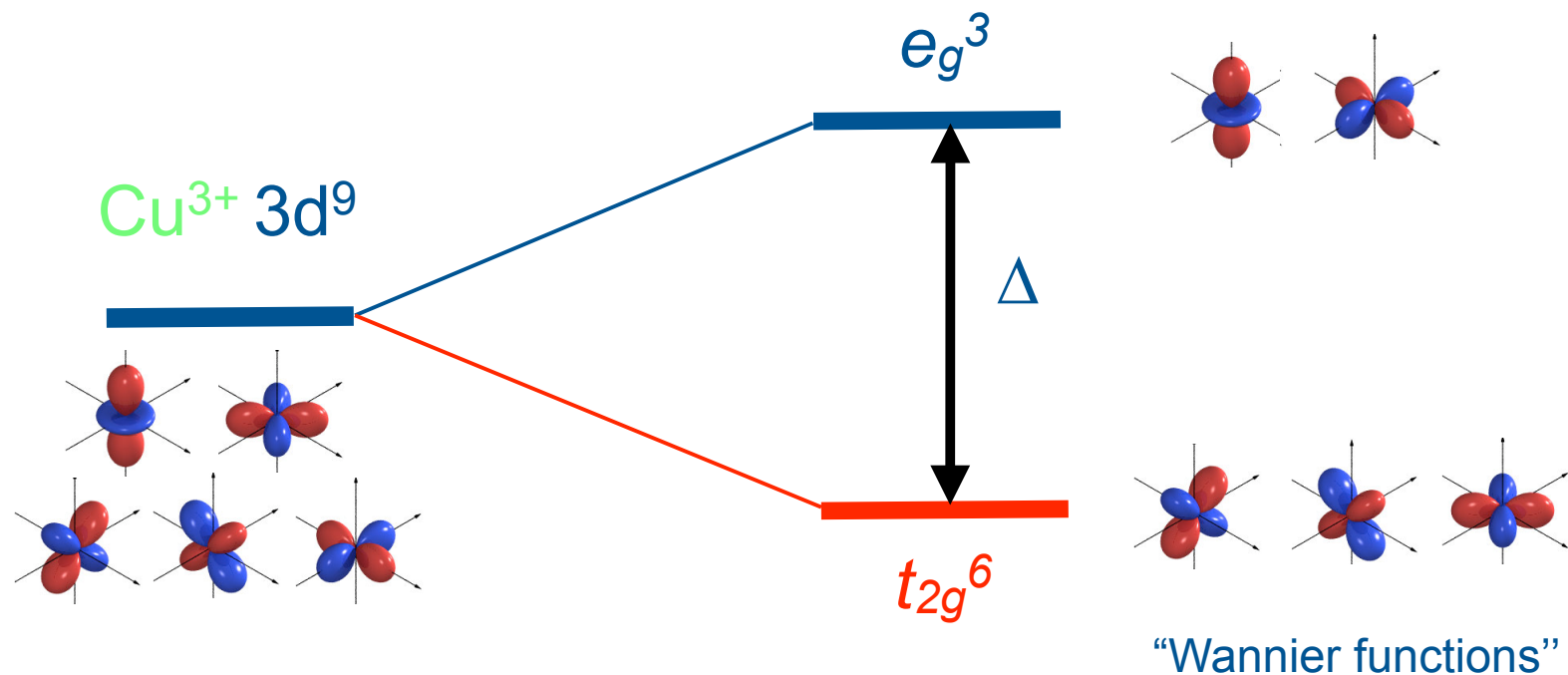
minimal material-specific model

minimal material-specific models

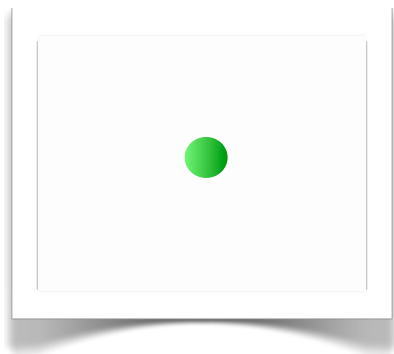
example: $3d^9$ cubic perovskite



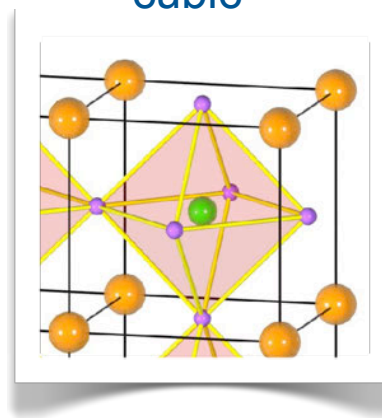
cubic crystal-field



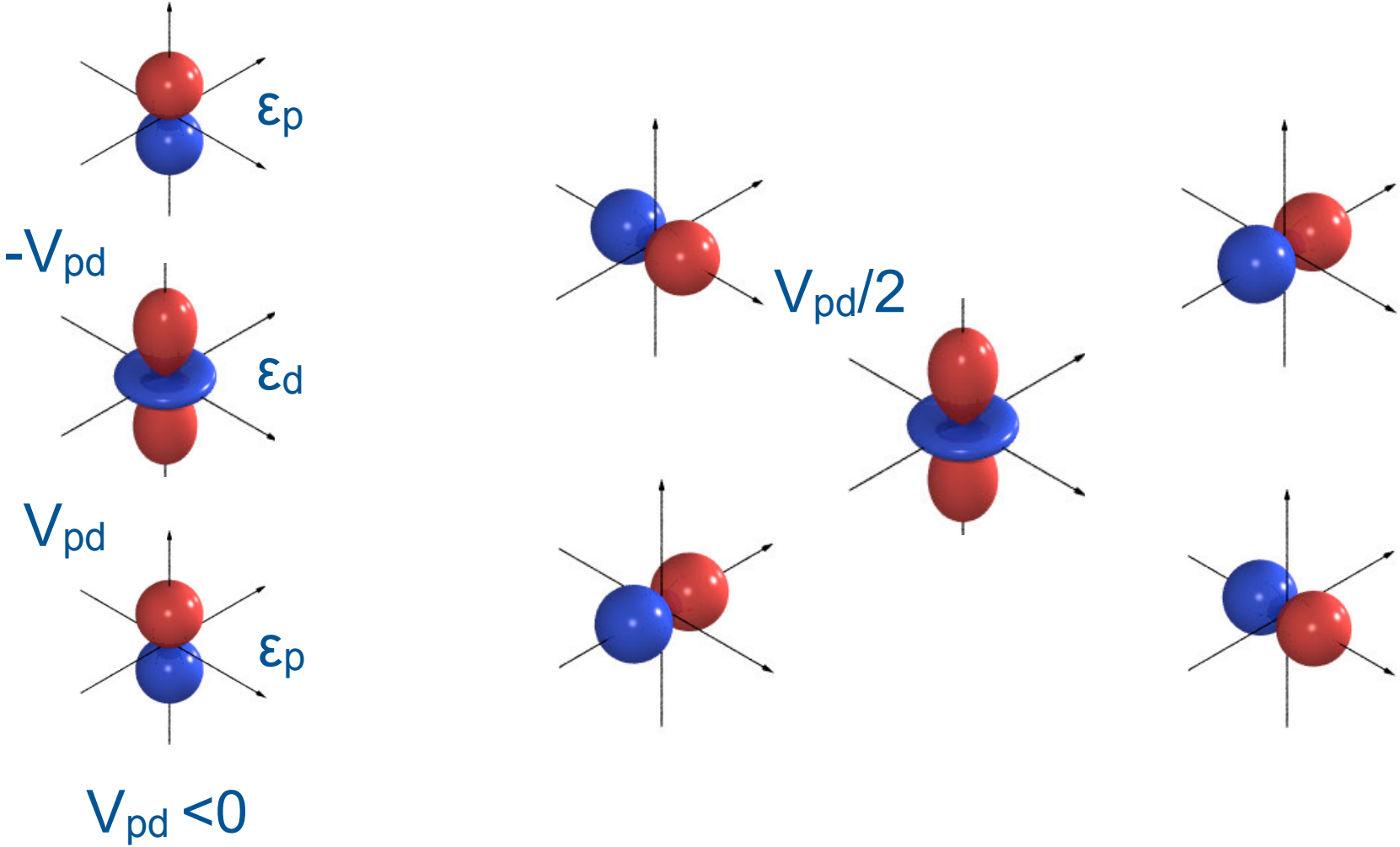
spherical



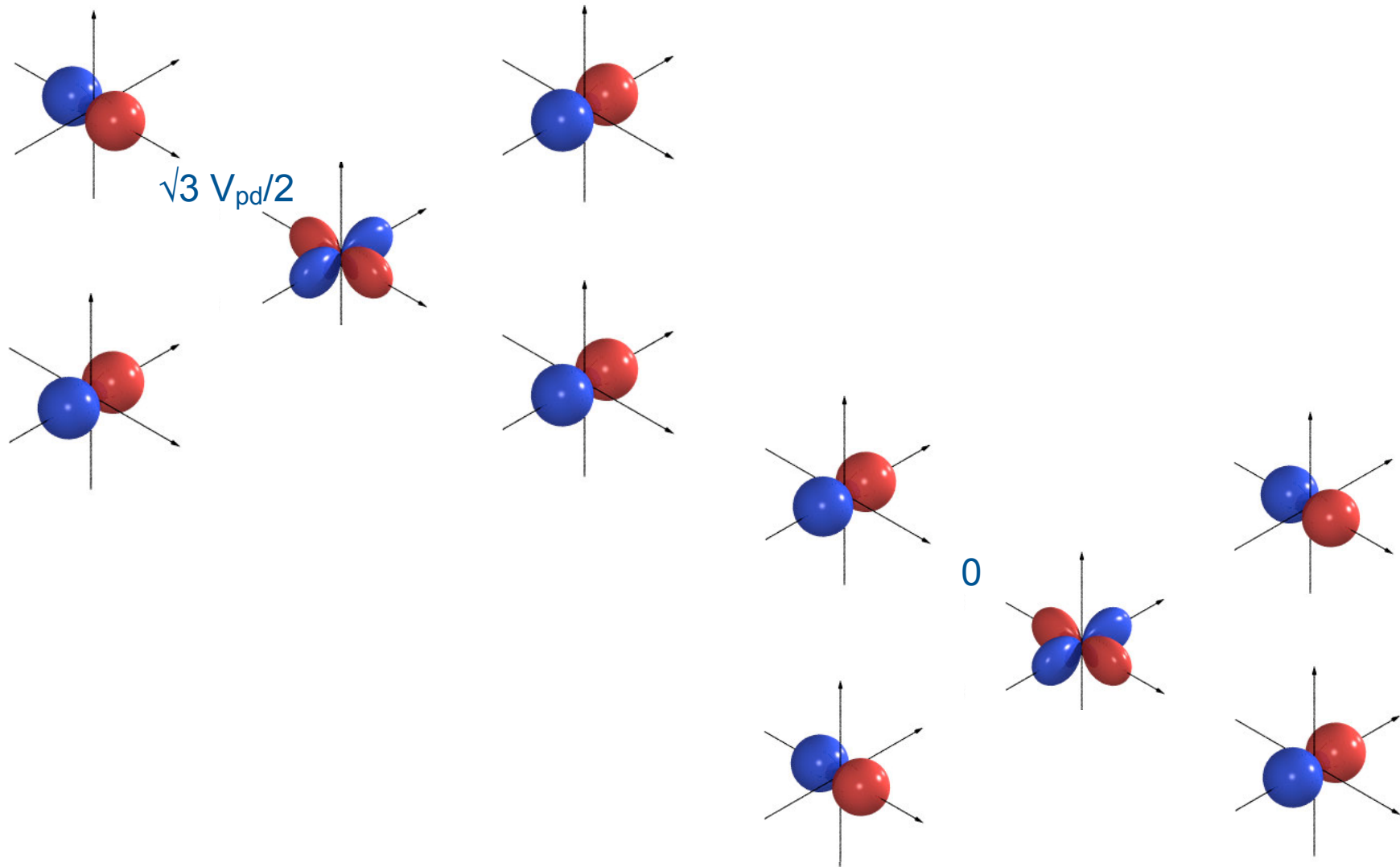
cubic



tight-binding model



tight-binding model



tight-binding model

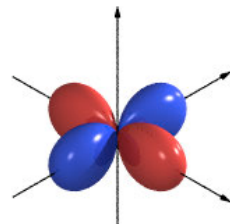
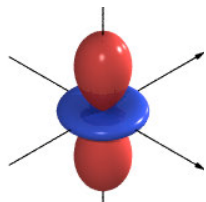
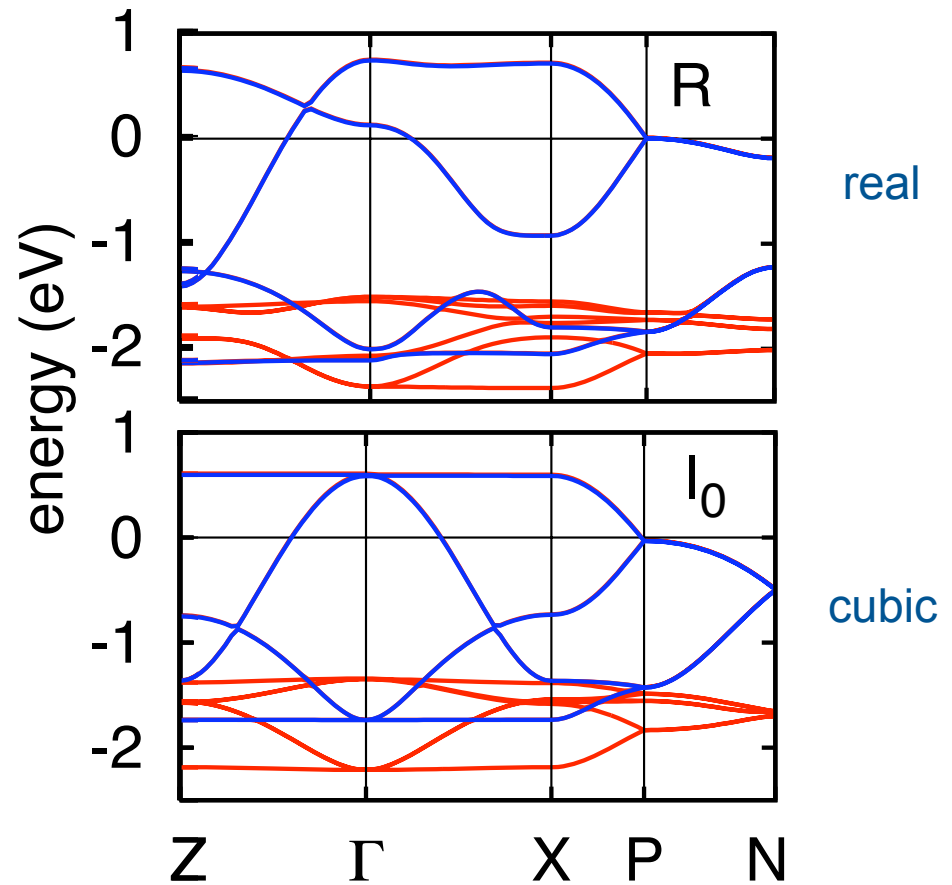
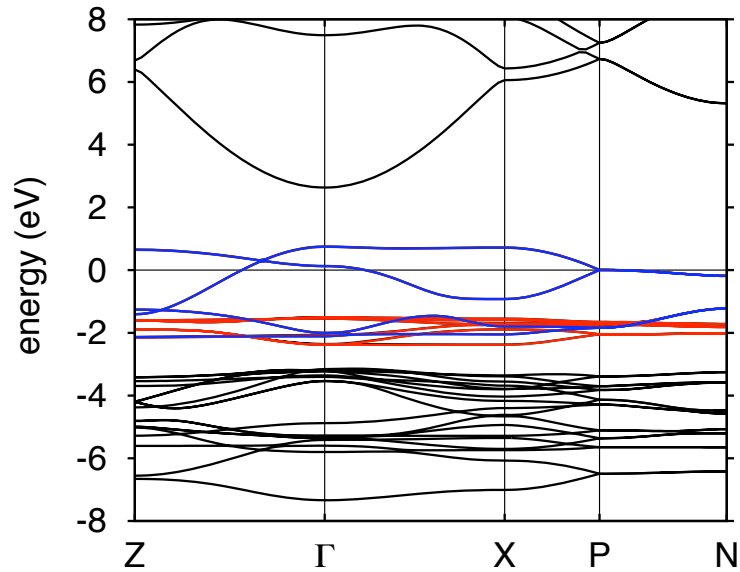
H^{TB}	$ \mathbf{k} z\rangle$	$ \mathbf{k} x\rangle$	$ \mathbf{k} y\rangle$	$ \mathbf{k} 3z^2 - r^2\rangle$	$ \mathbf{k} x^2 - y^2\rangle$
$ \mathbf{k} z\rangle$	ε_p	0	0	$-2V_{pd\sigma} s_z$	0
$ \mathbf{k} x\rangle$	0	ε_p	0	$V_{pd\sigma} s_x$	$-\sqrt{3}V_{pd\sigma} s_x$
$ \mathbf{k} y\rangle$	0	0	ε_p	$V_{pd\sigma} s_y$	$\sqrt{3}V_{pd\sigma} s_y$
$ \mathbf{k} 3z^2 - r^2\rangle$	$-2V_{pd\sigma} \bar{s}_z$	$V_{pd\sigma} \bar{s}_x$	$V_{pd\sigma} \bar{s}_y$	ε_d	0
$ \mathbf{k} x^2 - y^2\rangle$	0	$-\sqrt{3}V_{pd\sigma} \bar{s}_x$	$\sqrt{3}V_{pd\sigma} \bar{s}_y$	0	ε_d

$$s_\alpha = ie^{-ik_\alpha a/2} \sin k_\alpha a/2$$

from (0,0,0) to (0,0, π)

ε_2	=	ε_p		—	5
ε_3	=	ε_p		—	4
ε_4	=	ε_d		=	2,3
$\varepsilon_{1,5}$	=	$\varepsilon_p + \frac{1}{2}\Delta_{pd} \pm \frac{1}{2}\sqrt{\Delta_{pd}^2 + 16V_{pd\sigma}^2 s_z ^2}$		—	1

the e_g bands

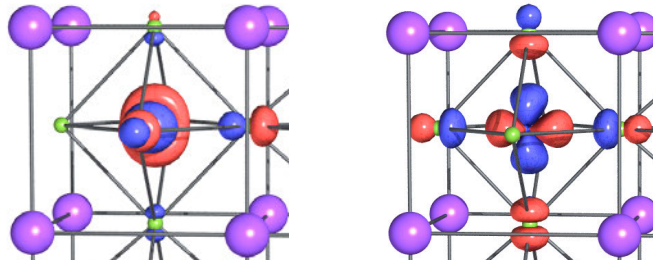


downfolding

$$\begin{bmatrix} H_{pp} & H_{pd} \\ H_{dp} & H_{dd} \end{bmatrix} \begin{bmatrix} |\mathbf{k} p\rangle \\ |\mathbf{k} d\rangle \end{bmatrix} = \varepsilon \begin{bmatrix} I_{pp} & 0 \\ 0 & I_{dd} \end{bmatrix} \begin{bmatrix} |\mathbf{k} p\rangle \\ |\mathbf{k} d\rangle \end{bmatrix}$$

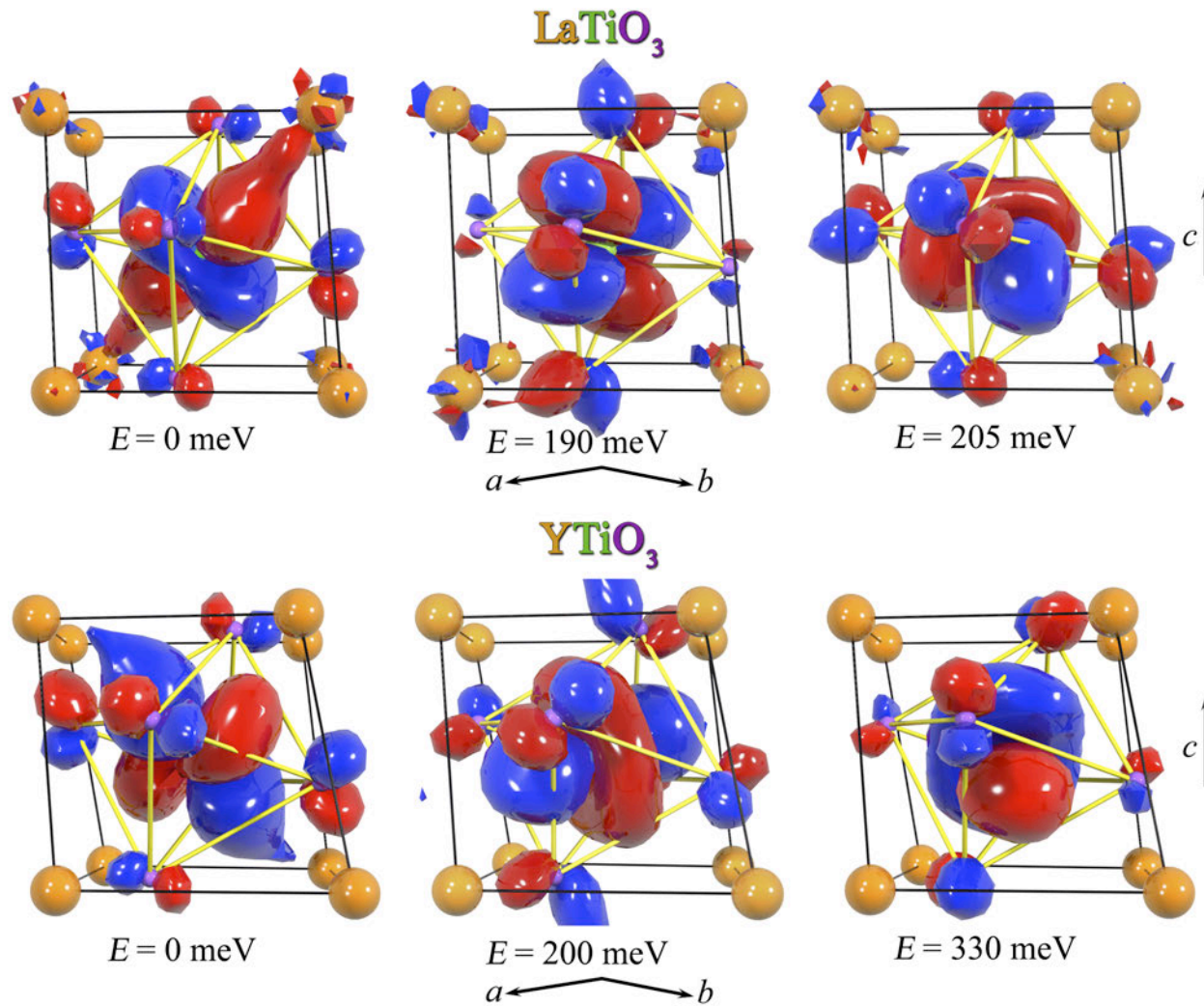
$$H_{dd}^\varepsilon = H_{dd} - H_{dp}(H_{pp} - \varepsilon I_{pp})^{-1}H_{pd},$$

H_{dd}^ε	$ \mathbf{k} 3z^2 - r^2\rangle_\varepsilon$	$ \mathbf{k} x^2 - y^2\rangle_\varepsilon$
$ \mathbf{k} 3z^2 - r^2\rangle_\varepsilon$	$\varepsilon'_d - 2t_\varepsilon \left[\frac{1}{4}(\cos k_x a + \cos k_y a) - \cos k_z a \right]$	$2t_\varepsilon \left[\frac{\sqrt{3}}{4}(\cos k_x a - \cos k_y a) \right]$
$ \mathbf{k} x^2 - y^2\rangle_\varepsilon$	$2t_\varepsilon \left[\frac{\sqrt{3}}{4}(\cos k_x a - \cos k_y a) \right]$	$\varepsilon'_d - 2t_\varepsilon \left[\frac{3}{4}(\cos k_x a + \cos k_y a) \right]$



ab-initio downfolding

NMTO Wannier functions



model for e_g (or t_{2g}) systems

$$\begin{aligned}
 H = & - \sum_{m,m',i,i',\sigma} t_{mm'}^{i,i'} c_{im\sigma}^\dagger c_{im'\sigma} + U \sum_{i,m} \hat{n}_{im\uparrow} \hat{n}_{im\downarrow} \\
 & + \frac{1}{2} \sum_{\substack{i\sigma\sigma' \\ m \neq m'}} (U - 2J - J\delta_{\sigma,\sigma'}) \hat{n}_{im\sigma} \hat{n}_{im'\sigma'} \\
 & - J \sum_{i,m \neq m'} \left[\underbrace{c_{im\uparrow}^\dagger c_{im\downarrow}^\dagger c_{im'\uparrow} c_{im'\downarrow}}_{\text{pair-hopping}} + \underbrace{c_{im\uparrow}^\dagger c_{im\downarrow} c_{im'\downarrow}^\dagger c_{im'\uparrow}}_{\text{spin-flip}} \right] - \hat{H}_{\text{DC}}^{e_g}
 \end{aligned}$$

$$U = U_0$$

$$J = J_2 \text{ or } J_1$$

methods of solution: LDA+*U*

Hartree-Fock and LDA+U

$$\hat{H}^{\text{LDA}} + \hat{U}^l - \hat{H}_{\text{DC}}^l = \hat{H}^{\text{LDA}} + \frac{1}{2}U \sum_i \sum_{m\sigma \neq m'\sigma'} \hat{n}_{im\sigma} \hat{n}_{im'\sigma'} - \frac{1}{2}U \sum_i \sum_{m\sigma \neq m'\sigma'} \langle \hat{n}_{im\sigma} \rangle \langle \hat{n}_{im'\sigma'} \rangle$$

Coulomb energy

Hartree part

$$\hat{n}_{im\sigma} \hat{n}_{im'\sigma'} \rightarrow \langle \hat{n}_{im\sigma} \rangle \hat{n}_{im'\sigma'} + \hat{n}_{im\sigma} \langle \hat{n}_{im'\sigma'} \rangle - \langle \hat{n}_{im\sigma} \rangle \langle \hat{n}_{im'\sigma'} \rangle$$

mean-field (Hartree-like)

$$H = \hat{H}^{\text{LDA}} + \sum_{im\sigma} t_m^\sigma \hat{n}_{im\sigma}, \quad \text{with} \quad t_m^\sigma = U \left(\frac{1}{2} - \langle \hat{n}_{im\sigma} \rangle \right)$$

+U/2

-U/2

$$E_{\text{LDA+U}}[n] = E_{\text{LDA}}[n] + \sum_i \left[\frac{1}{2}U \sum_{m\sigma \neq m'\sigma'} \langle \hat{n}_{im\sigma} \rangle \langle \hat{n}_{im'\sigma'} \rangle - E_{\text{DC}} \right]$$

$$\varepsilon_{im\sigma}^{\text{LDA+U}} = \frac{\partial E_{\text{LDA+U}}}{\partial \langle \hat{n}_{im\sigma} \rangle} = \varepsilon_{im\sigma}^{\text{LDA}} + U \left(\frac{1}{2} - \langle \hat{n}_{im\sigma} \rangle \right)$$

charge self-consistent

generalization

$$\begin{aligned}
 E_{\text{LDA+U}}[n] &= E_{\text{LDA}}[n] + \frac{1}{2} \sum_{i\sigma} \sum_{mm'm''m'''} U_{mm'm''m'''} \langle \hat{n}_{im m'}^\sigma \rangle \langle \hat{n}_{im''m'''}^{-\sigma} \rangle \\
 &+ \frac{1}{2} \sum_{i\sigma} \sum_{mm'm''m'''} [U_{mm'm''m'''} - U_{mm''m''m'}] \langle \hat{n}_{im m'}^\sigma \rangle \langle \hat{n}_{im''m'''}^\sigma \rangle - E_{\text{DC}}
 \end{aligned}$$

$$E_{\text{DC}} = \frac{1}{2} U_{\text{avg}} N^l (N^l - 1) - \frac{1}{2} J_{\text{avg}} \sum_{\sigma} N_{\sigma}^l (N_{\sigma}^l - 1)$$

$$\hat{H} = \hat{H}^{\text{LDA}} + \sum_{imm'\sigma} t_{mm'}^{\sigma} c_{im\sigma}^{\dagger} c_{im'\sigma}$$

$$\begin{aligned}
 t_{mm'}^{\sigma} &= \sum_{i\sigma} \sum_{m''m'''} U_{mm''m''m'''} \langle \hat{n}_{im''m'''}^{-\sigma} \rangle + [U_{mm''m''m'''} - U_{mm''m''m'}] \langle \hat{n}_{im''m'''}^{\sigma} \rangle \\
 &- \left[U_{\text{avg}} \left(N^l - \frac{1}{2} \right) - J_{\text{avg}} \left(N_{\sigma}^l - \frac{1}{2} \right) \right] \delta_{m,m'}
 \end{aligned}$$

LDA+U for a e_g model

$$\begin{aligned}
 H = & - \sum_{m,m',i,i',\sigma} t_{mm'}^{i,i'} c_{im\sigma}^\dagger c_{im'\sigma} + U \sum_{i,m} \hat{n}_{im\uparrow} \hat{n}_{im\downarrow} \\
 & + \frac{1}{2} \sum_{\substack{i\sigma\sigma' \\ m \neq m'}} (U - 2J - J\delta_{\sigma,\sigma'}) \hat{n}_{im\sigma} \hat{n}_{im'\sigma'} \\
 & - J \sum_{i,m \neq m'} \left[c_{im\uparrow}^\dagger c_{im\downarrow}^\dagger c_{im'\uparrow} c_{im'\downarrow} + c_{im\uparrow}^\dagger c_{im\downarrow} c_{im'\downarrow}^\dagger c_{im'\uparrow} \right] - \hat{H}_{DC}^{e_g}
 \end{aligned}$$

$$\Sigma^{i\sigma} = \begin{bmatrix} \Sigma_{\alpha,\alpha}^{i\sigma} & \Sigma_{\alpha,\beta}^{i\sigma} \\ \Sigma_{\beta,\alpha}^{i\sigma} & \Sigma_{\beta,\beta}^{i\sigma} \end{bmatrix}$$

at site i

$$\Sigma^{i\sigma} = U \begin{bmatrix} \frac{1}{2} - \langle \hat{n}_{i\alpha\alpha}^\sigma \rangle & -\langle \hat{n}_{i\beta\alpha}^\sigma \rangle \\ -\langle \hat{n}_{i\alpha\beta}^\sigma \rangle & \frac{1}{2} - \langle \hat{n}_{i\beta\beta}^\sigma \rangle \end{bmatrix}$$

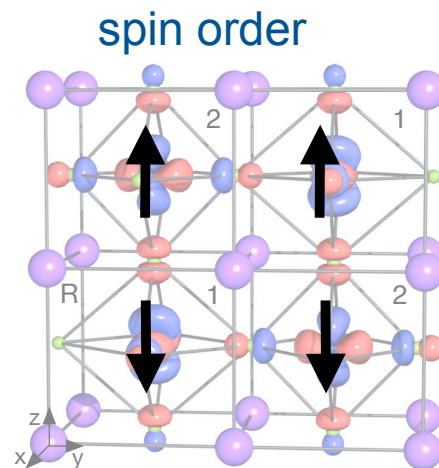
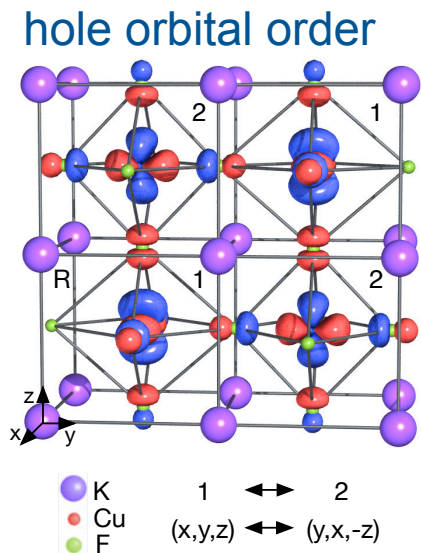
LDA+U, $J=0$

other sites: symmetries!

only correlated electrons: double counting incorporated in chemical potential

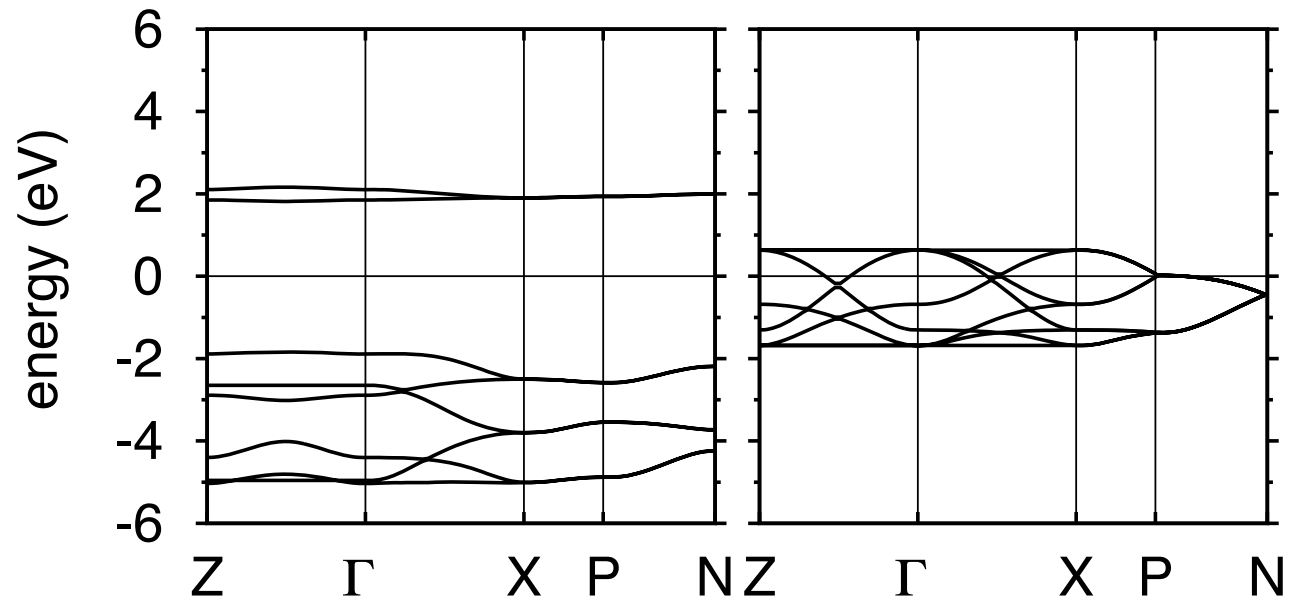
$$E_{DC} = \frac{1}{2} U_{avg} N^l (N^l - 1) - \frac{1}{2} J_{avg} \sum_{\sigma} N_{\sigma}^l (N_{\sigma}^l - 1)$$

KCuF₃



Σ/U	$ \alpha\sigma\rangle_{1u}$	$ \beta\sigma\rangle_{1u}$	$ \alpha\sigma\rangle_{2u}$	$ \beta\sigma\rangle_{2u}$	$ \alpha\sigma\rangle_{1d}$	$ \beta\sigma\rangle_{1d}$	$ \alpha\sigma\rangle_{2d}$	$ \beta\sigma\rangle_{2d}$
$ \alpha\sigma\rangle_{1u}$	$\frac{-2\delta_{\sigma,\downarrow} - \delta_{\sigma,\uparrow}}{4}$	$\frac{\sqrt{3}\delta_{\sigma,\uparrow}}{4}$	0	0	0	0	0	0
$ \beta\sigma\rangle_{1u}$	$\frac{\sqrt{3}\delta_{\sigma,\uparrow}}{4}$	$\frac{-2\delta_{\sigma,\downarrow} + \delta_{\sigma,\uparrow}}{4}$	0	0	0	0	0	0
$ \alpha\sigma\rangle_{2u}$	0	0	$\frac{-2\delta_{\sigma,\downarrow} - \delta_{\sigma,\uparrow}}{4}$	$\frac{-\sqrt{3}\delta_{\sigma,\uparrow}}{4}$	0	0	0	0
$ \beta\sigma\rangle_{2u}$	0	0	$\frac{-\sqrt{3}\delta_{\sigma,\uparrow}}{4}$	$\frac{-2\delta_{\sigma,\downarrow} + \delta_{\sigma,\uparrow}}{4}$	0	0	0	0
$ \alpha\sigma\rangle_{1d}$	0	0	0	0	$\frac{-2\delta_{\sigma,\uparrow} - \delta_{\sigma,\downarrow}}{4}$	$\frac{\sqrt{3}\delta_{\sigma,\downarrow}}{4}$	0	0
$ \beta\sigma\rangle_{1d}$	0	0	0	0	$\frac{\sqrt{3}\delta_{\sigma,\downarrow}}{4}$	$\frac{-2\delta_{\sigma,\uparrow} + \delta_{\sigma,\downarrow}}{4}$	0	0
$ \alpha\sigma\rangle_{2d}$	0	0	0	0	0	0	$\frac{-2\delta_{\sigma,\uparrow} - \delta_{\sigma,\downarrow}}{4}$	$\frac{-\sqrt{3}\delta_{\sigma,\downarrow}}{4}$
$ \beta\sigma\rangle_{2d}$	0	0	0	0	0	0	$\frac{-\sqrt{3}\delta_{\sigma,\downarrow}}{4}$	$\frac{-2\delta_{\sigma,\uparrow} + \delta_{\sigma,\downarrow}}{4}$

LDA+ U bands

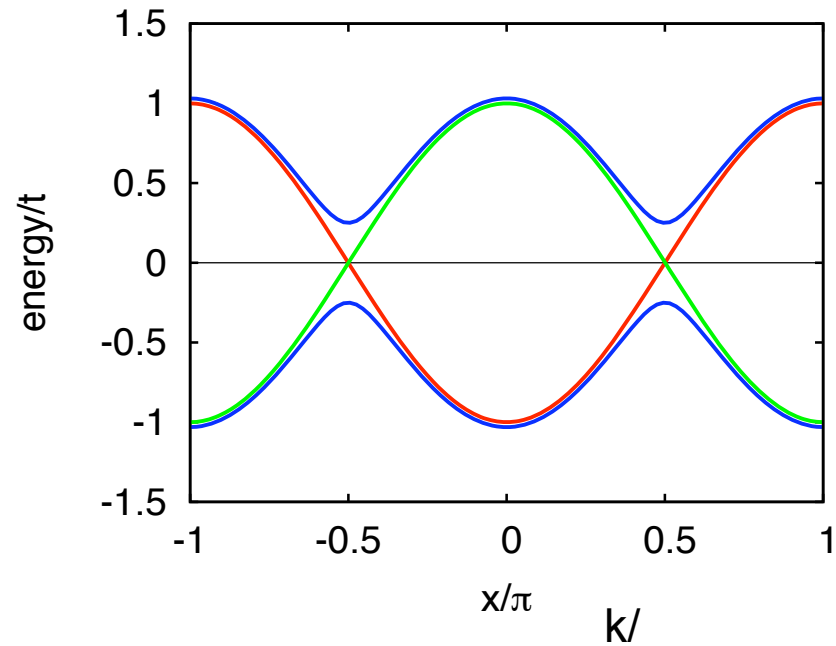


LDA+ U e_g bands
(no charge self-consistency)

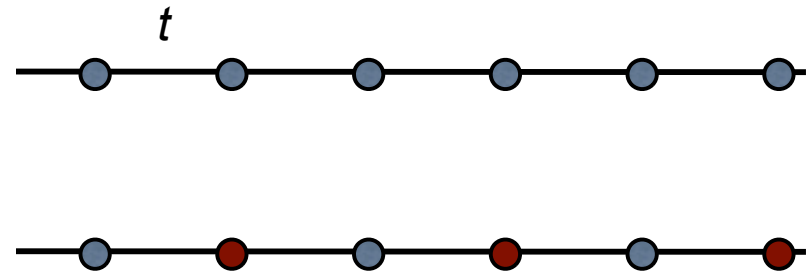
lda e_g bands
supercell 4 formula units

infinite lifetime and static self-energy

AFM linear Hubbard chain



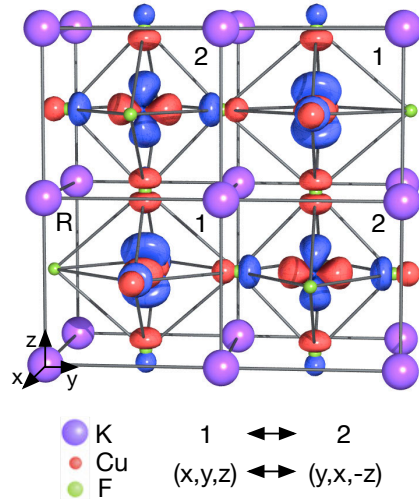
AFM: double cell, half BZ



$$\hat{H} = -t \sum_{\sigma \langle ii' \rangle} c_{i\sigma}^\dagger c_{i'\sigma} + U \sum_i \hat{n}_{i\uparrow} \hat{n}_{i\downarrow} = \hat{H}_0 + \hat{U}$$

methods of solution: LDA+DMFT

KCuF₃



paramagnetic

massive downfolding to e_g

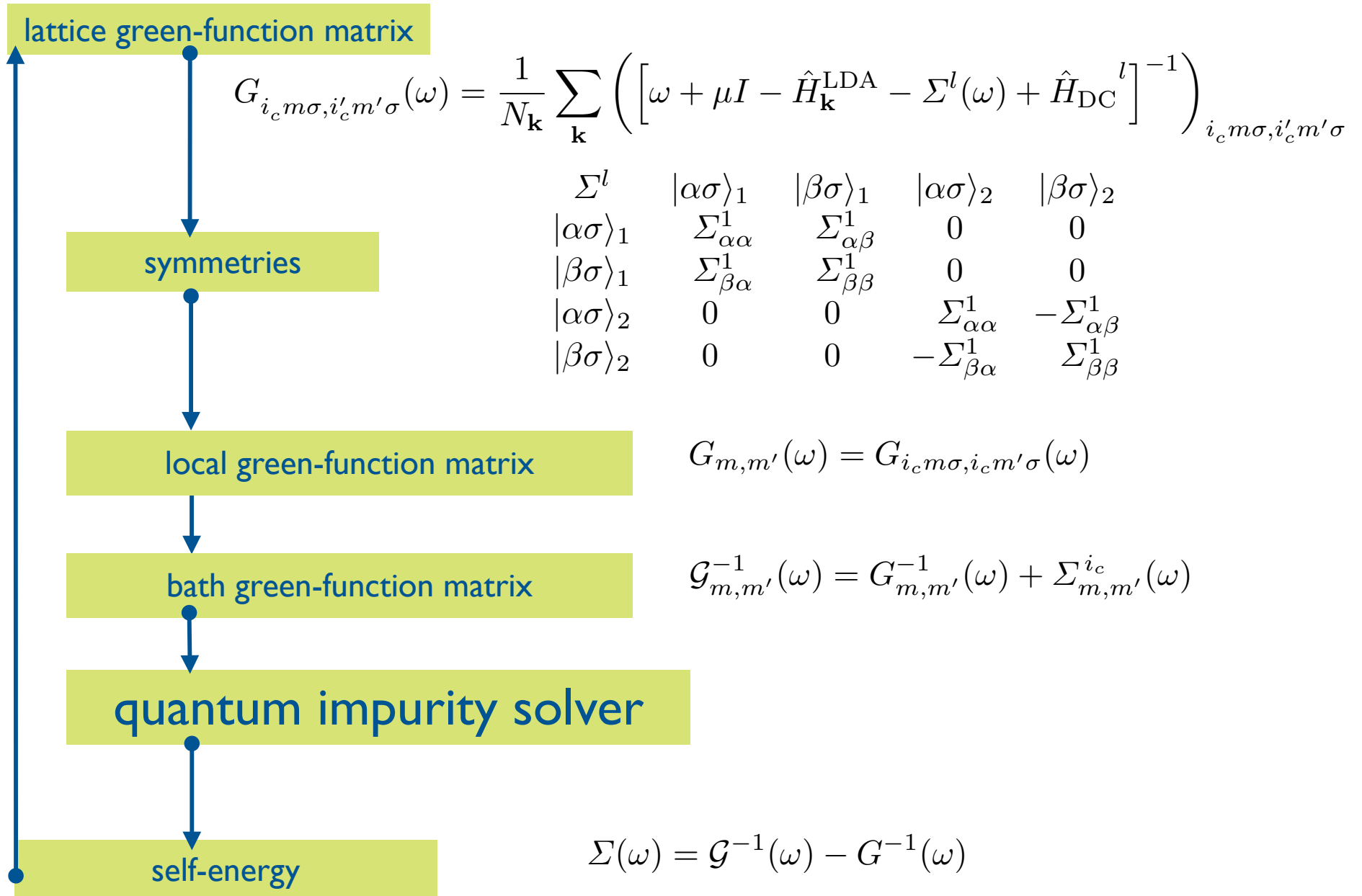
H_{dd}^ε	$ \mathbf{k} 3z^2 - r^2\rangle_\varepsilon$	$ \mathbf{k} x^2 - y^2\rangle_\varepsilon$
$ \mathbf{k} 3z^2 - r^2\rangle_\varepsilon$	$\varepsilon'_d - 2t_\varepsilon \left[\frac{1}{4} (\cos k_x a + \cos k_y a) - \cos k_z a \right]$	$2t_\varepsilon \left[\frac{\sqrt{3}}{4} (\cos k_x a - \cos k_y a) \right]$
$ \mathbf{k} x^2 - y^2\rangle_\varepsilon$	$2t_\varepsilon \left[\frac{\sqrt{3}}{4} (\cos k_x a - \cos k_y a) \right]$	$\varepsilon'_d - 2t_\varepsilon \left[\frac{3}{4} (\cos k_x a + \cos k_y a) \right]$

e_g H^{LDA}

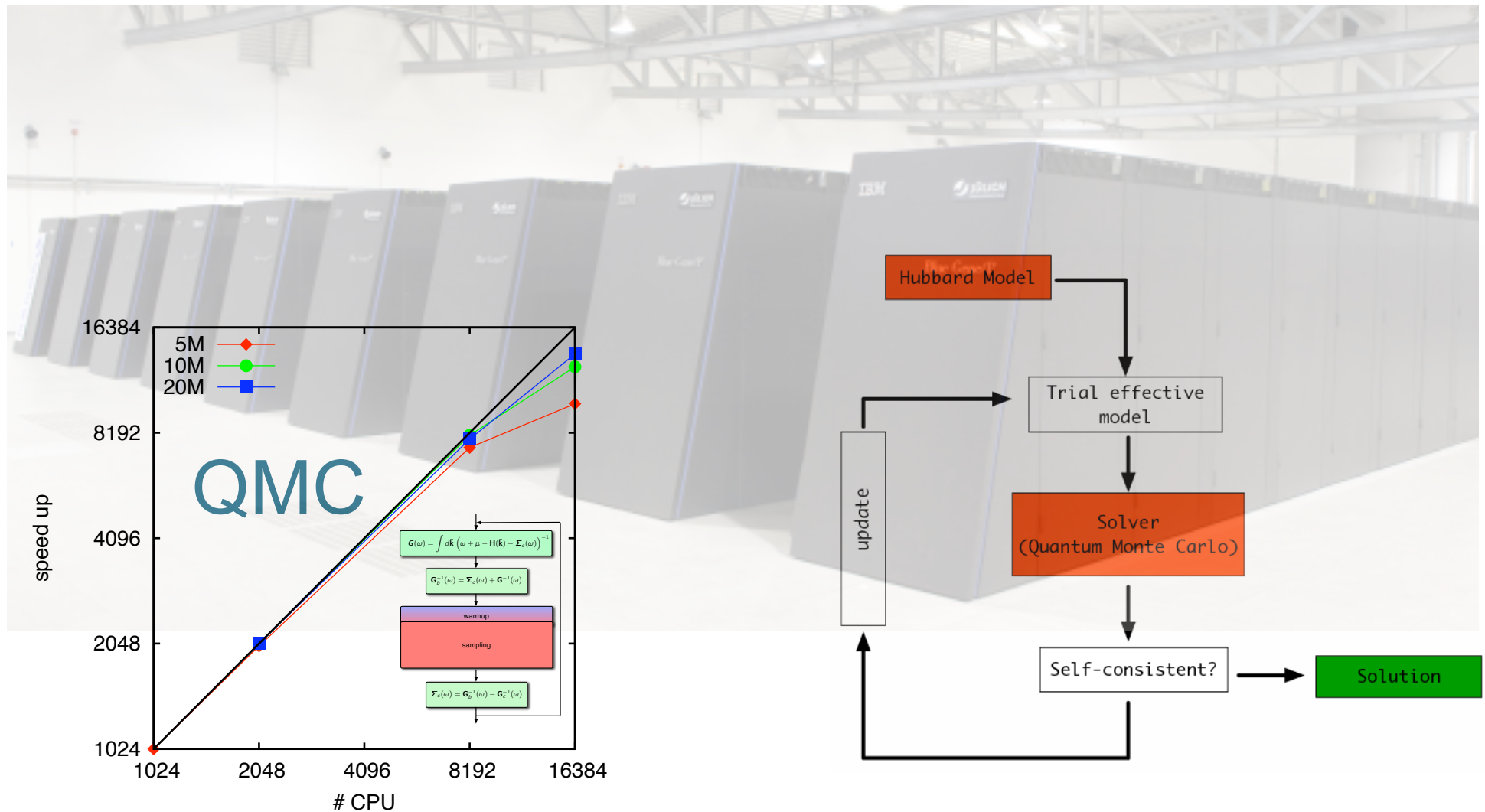
2 equivalent sites

Σ^l	$ \alpha\sigma\rangle_1$	$ \beta\sigma\rangle_1$	$ \alpha\sigma\rangle_2$	$ \beta\sigma\rangle_2$
$ \alpha\sigma\rangle_1$	$\Sigma_{\alpha\alpha}^1$	$\Sigma_{\alpha\beta}^1$	0	0
$ \beta\sigma\rangle_1$	$\Sigma_{\beta\alpha}^1$	$\Sigma_{\beta\beta}^1$	0	0
$ \alpha\sigma\rangle_2$	0	0	$\Sigma_{\alpha\alpha}^1$	$-\Sigma_{\alpha\beta}^1$
$ \beta\sigma\rangle_2$	0	0	$-\Sigma_{\beta\alpha}^1$	$\Sigma_{\beta\beta}^1$

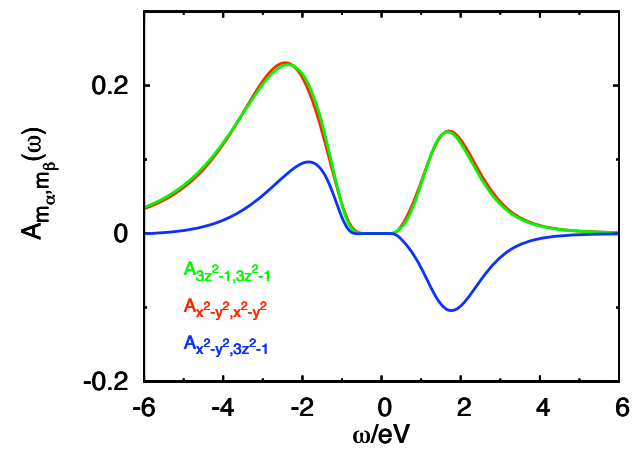
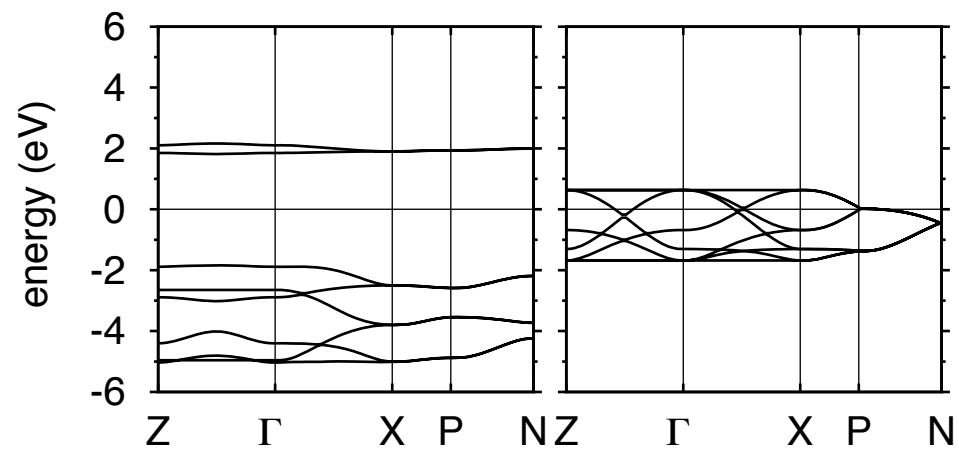
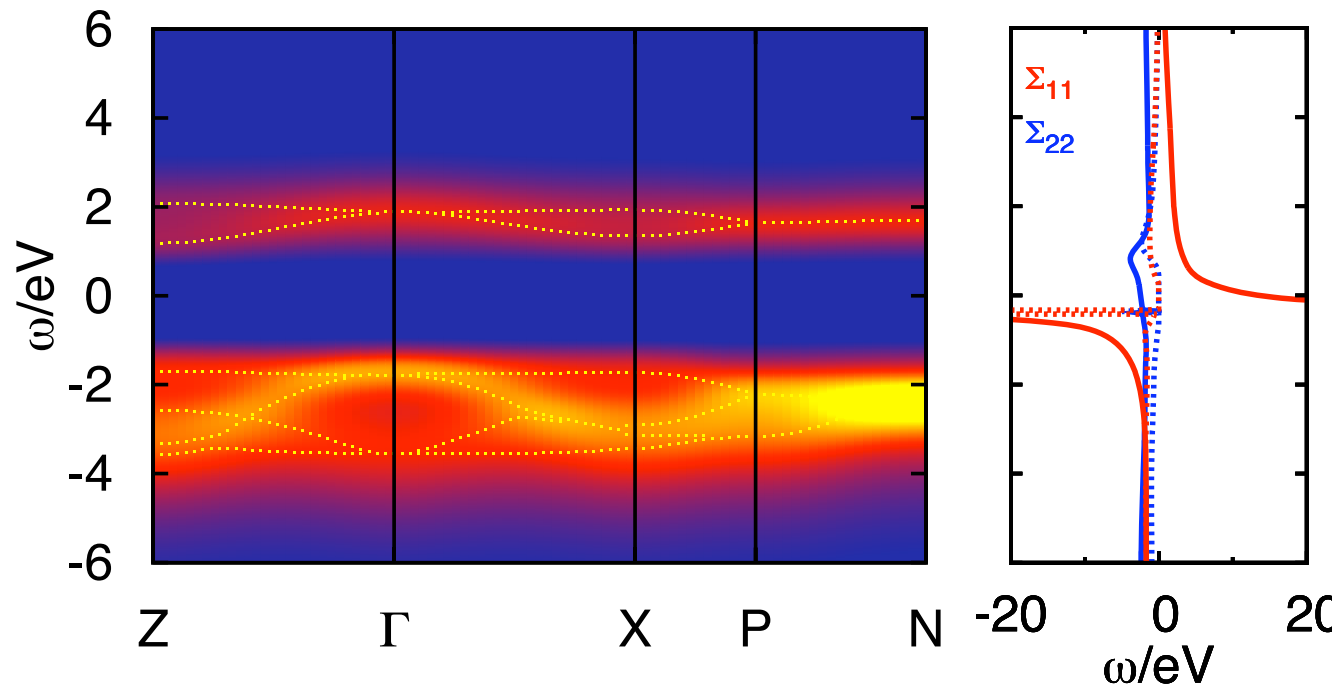
paramagnetic LDA+DMFT



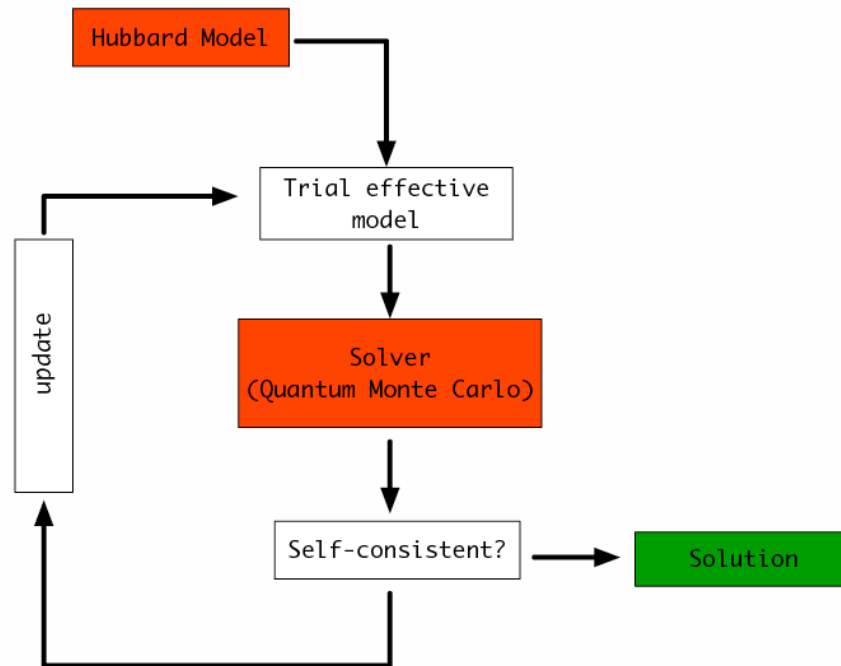
quantum impurity solvers



KCuF₃



extensions

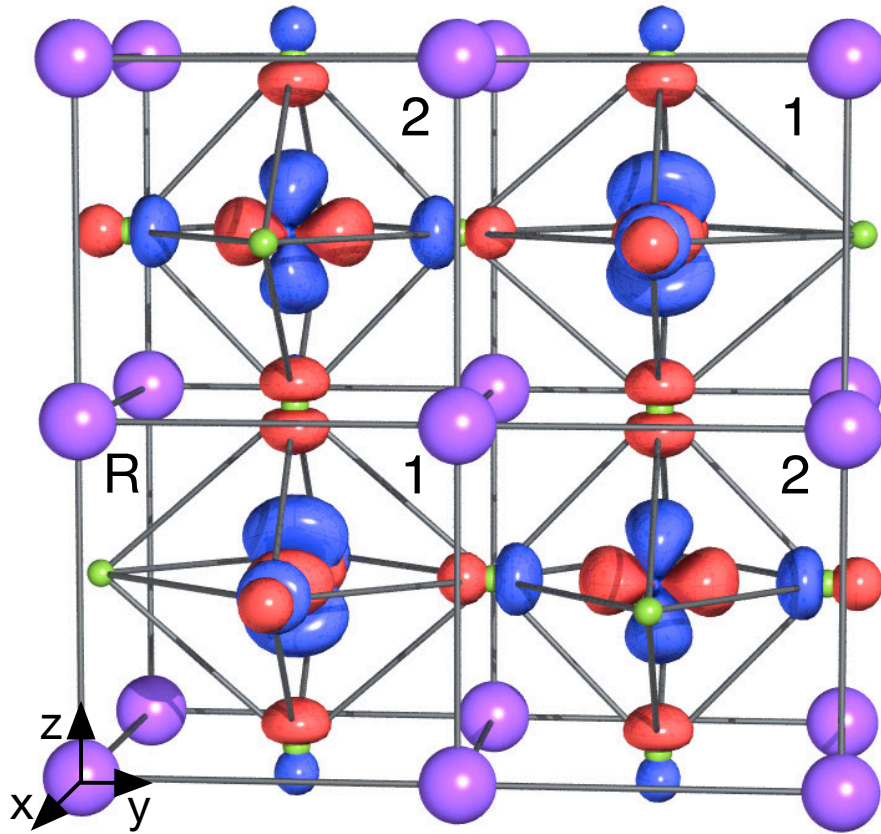


- ferro and anti ferro magnetism
- charge self-consistency
- cluster DMFT
- GW+DMFT
-

example: orbital order in KCuF_3

orbital order in KCuF_3

problem to solve: why a co-operative Jahn-Teller distortion?



Orbital Order

CORRELATED ELECTRON SYSTEMS
REVIEW

Orbital Physics in Transition-Metal Oxides

Y. Tokura^{1,2} and N. Nagaosa¹

An electron in a solid, that is, bound to or nearly localized on the specific atomic site, has three attributes: charge, spin, and orbital. The orbital represents the shape of the electron cloud in solid. In transition-metal oxides with anisotropic-shaped d-orbital electrons, the Coulomb interaction between the electrons (strong electron correlation effect) is of importance for understanding their metal-insulator transitions and properties such as high-temperature superconductivity and colossal magnetoresistance. The orbital degree of freedom occasionally plays an important role in these phenomena, and its correlation and/or order-disorder transition causes a variety of phenomena through strong coupling with charge, spin, and lattice dynamics. An overview is given here on this "orbital physics," which will be a key concept for the science and technology of correlated electrons.

When more than two orbitals are involved, a variety of situations can be realized, and this quantum mechanical process depends on the orbitals (d, f). In this way, the spin \vec{S} and the orbital pseudospin \vec{T} are coupled. In more general cases, the transfer integral t_{ij} depends on the direction of the bond ij and also on the pair of the two orbitals $a, b = (x^2 - y^2)$ or $(3z^2 - r^2)$. This gives rise to the anisotropy of the Hamiltonian in the pseudospin space as well as in the real space. For example, the transfer integral between the two neighboring Mn atoms in the crystal lattice is determined

309

Electronic reconstruction at an interface between a Mott insulator and a band insulator

Satoshi Okamoto & Andrew J. Millis

Department of Physics, Columbia University 538 West 120th Street, New York, New York 10027, USA

Surface science is an important and well-established branch of materials science involving the study of changes in material

NEWS & VIEWS

TRANSITION METAL OXIDES

Ferroelectricity driven by orbital order

The discovery that the rotation of the orbital arrangement in manganites induces ferroelectricity exposes an intriguing phase transition that could serve as a blueprint for novel applications.

BERNHARD KEIMER

is at the Max Planck Institute for Solid State Research, Heisenbergstr. 1, 70569 Stuttgart, Germany
e-mail: B.Keimer@fkf.mpg.de

Transition metal oxides have fascinated scientists since the 1950s, when the newly developed technique of neutron diffraction was used to show that the compound $\text{La}_{1-x}\text{Ca}_x\text{MnO}_3$ exhibits a rich variety of structural and magnetic phases as the Ca concentration is tuned. The fascination has increased in the wake of the discovery of high-temperature superconductivity in a chemically similar compound.



Figure 1 Possible arrangements of Mn^{2+} d -orbitals on a square lattice. The patterns are two-dimensional versions of orbitally ordered states actually observed in manganese oxides. The corresponding magnetic states are indicated by yellow arrows.

Ionic relaxation contribution to the electronic reconstruction at the n -type $\text{LaAlO}_3/\text{SrTiO}_3$ interface

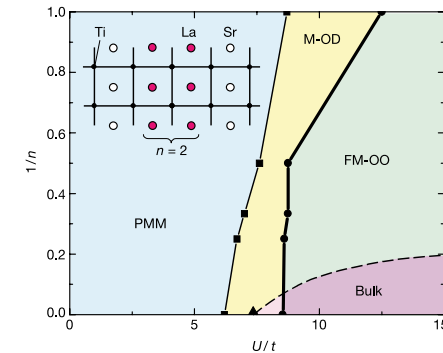
Rossitza Pentcheva¹ and Warren E. Pickett²

¹Department of Earth and Environmental Sciences, University of Munich, Theresienstr 41, 80333 Munich, Germany

²Department of Physics, University of California, Davis, California 95616, USA

(Received 30 June 2008; revised manuscript received 19 September 2008; published 7 November 2008)

Density-functional theory calculations reveal that the compensation mechanism at the isolated n -type interface in $\text{LaAlO}_3/\text{SrTiO}_3$ superlattices involves both ionic and electronic degrees of freedom. Strong polar distortions screen the local electric field and reduce the band discontinuity across the interface. We find that the electronic reconstruction depends sensitively on whether structural optimization is performed within GGA (conventional exchange and correlation effects) or $\text{GGA}+U$ (which includes strong intra-atomic interactions). For a structural optimization within $\text{GGA}+U$ the excess charge is confined to the interface TiO_2 layer with a charge-ordered, orbitally polarized arrangement of Ti^{3+} and Ti^{4+} . While the charge-ordered phase represents the ground state, optimization within GGA leads to more pronounced lattice polarization, suppression of charge order (with remaining d_{xy} -orbital occupation in the interface layer), and a delocalization of the excess charge



PHYSICAL REVIEW B 78, 201102(R) (2008)

Magnetism, conductivity, and orbital order in $(\text{LaMnO}_3)_{2n}/(\text{SrMnO}_3)_n$ superlattices

Shuai Dong,^{1,2,3} Rong Yu,^{1,2} Seiji Yunoki,^{4,5} Gonzalo Alvarez,⁶ J.-M. Liu,³ and Elbio Dagotto^{1,2}

¹Department of Physics and Astronomy, University of Tennessee, Knoxville, Tennessee 37996, USA

²Materials Science and Technology Division, Oak Ridge National Laboratory, Oak Ridge, Tennessee 32831, USA

³Nanjing National Laboratory of Microstructures, Nanjing University, Nanjing 210093, China

⁴Computational Condensed Matter Physics Laboratory, RIKEN, Wako, Saitama 351-0198, Japan

⁵CREST, Japan Science and Technology Agency (JST), Kawaguchi, Saitama 332-0012, Japan

⁶Computer Science and Mathematics Division and Center for Nanophase Materials Science, Oak Ridge National Laboratory, Oak Ridge, Tennessee 37831, USA

(Received 8 October 2008; published 21 November 2008)

The modulation of charge density and spin order in $(\text{LaMnO}_3)_{2n}/(\text{SrMnO}_3)_n$ ($n=1-4$) superlattices is studied via Monte Carlo simulations of the double-exchange model. G -type antiferromagnetic barriers in the

electron-phonon coupling

Crystal Distortion in Magnetic Compounds

JUNJIRO KANAMORI*

Institute for the Study of Metals, University of Chicago, Chicago 37, Illinois

The crystal distortion which arises from the Jahn-Teller effect is discussed in several examples. In the case of compounds containing Cu^{2+} or Mn^{3+} at octahedral sites, the lowest orbital level of these ions is doubly degenerate in the undistorted structure, and there is no spin-orbit coupling in this level. It is shown that, introducing a fictitious spin to specify the degenerate orbital states, we can discuss the problem by analogy with the magnetic problems. The "ferromagnetic" and "antiferromagnetic" distortions are discussed in detail. The transition from the distorted to the undistorted structure is of the first kind for the former and of the second kind for the latter. Higher approximations are discussed briefly. In compounds like FeO , CoO , and CuCr_2O_4 , the lowest orbital level is triply degenerate, and the spin-orbit coupling is present in this level. In this case the distortion is dependent on the magnitude of the spin-orbit coupling relative to the strength of the Jahn-Teller effect term. The distortion at absolute zero temperature and its temperature dependence are discussed.

$$H_1 = -g\sqrt{C}(\sigma_z Q_3 + \sigma_x Q_2)$$

$$\frac{E_0 + \Delta/2}{E_0 - \Delta/2} = \frac{\Delta}{\theta}$$

$$|\theta\rangle = \sin \frac{\theta}{2} |3z^2 - 1\rangle + \cos \frac{\theta}{2} |x^2 - y^2\rangle$$

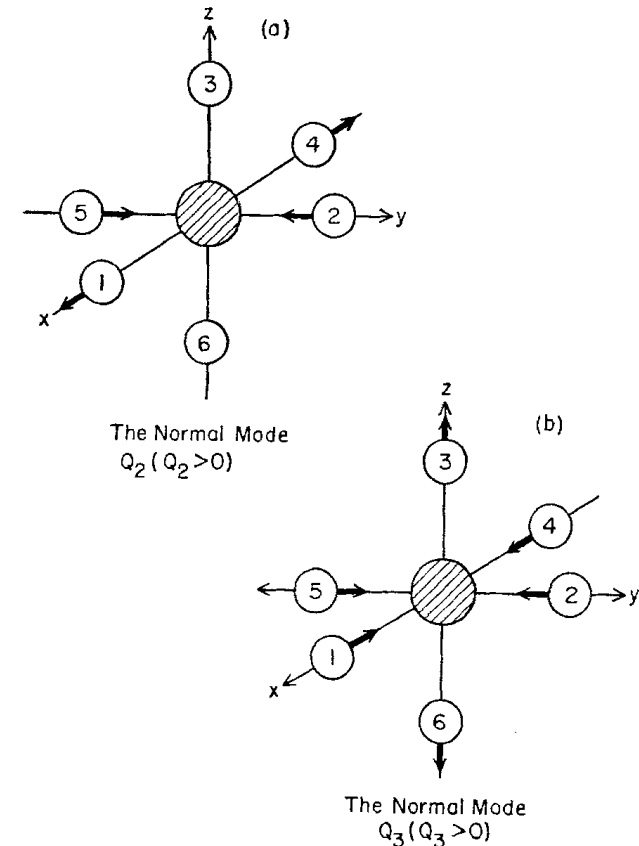


FIG. 2. (a) The normal mode Q_2 ($Q_2 > 0$).
(b) The normal mode Q_3 ($Q_3 > 0$).

do we need a large crystal-field?

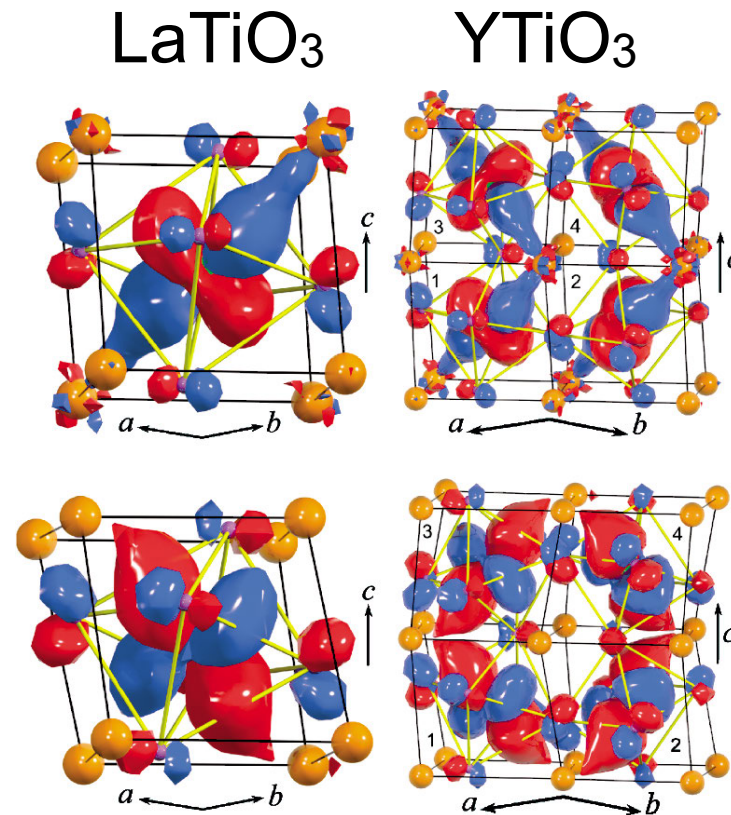
VOLUME 92, NUMBER 17

PHYSICAL REVIEW LETTERS

week ending
30 APRIL 2004

Mott Transition and Suppression of Orbital Fluctuations in Orthorhombic $3d^1$ Perovskites

E. Pavarini,¹ S. Biermann,² A. Poteryaev,³ A. I. Lichtenstein,³ A. Georges,² and O. K. Andersen⁴



LDA+DMFT 770 K
 $\Delta=200-300$ meV

a 100 meV crystal-field could be enough

super-exchange

Crystal structure and magnetic properties of substances with orbital degeneracy

K. I. Kugel' and D. I. Khomskii'

P. N. Lebedev Physics Institute

(Submitted November 13, 1972)

Zh. Eksp. Teor. Fiz. **64**, 1429-1439 (April 1973)

Exchange interaction in magnetic substances containing ions with orbital degeneracy is considered. It is shown that, among with spin ordering, superexchange also results in cooperative ordering of Jahn-Teller ion orbitals, which, generally speaking, occurs at a higher temperature and is accompanied by distortion of the lattice (which is a secondary effect here). Concrete studies are performed for substances with a perovskite structure (KCuF₃, LaMnO₃, MnF₃). The effective spin Hamiltonian is obtained for these substances and the properties of the ground state are investigated. The orbital and magnetic structures obtained in this way without taking into account interaction with the lattice are in accord with the structures observed experimentally. The approach employed also permits one to explain the strong anisotropy of the magnetic properties of these compounds and to obtain a reasonable estimate for the critical temperatures.

$$H = - \sum_{imjm'\sigma} t_{imjm'} c_{im\sigma}^\dagger c_{jm'\sigma} + U \sum_{im\sigma jm'\sigma'} n_{im\sigma} n_{jm'\sigma'}$$

perturbation t/U \longrightarrow super-exchange Hamiltonian

$$H = J_{ss} \mathbf{S}_i \cdot \mathbf{S}_j + J_{oo} \mathbf{Q}_i \mathbf{Q}_j + J_{so} \mathbf{Q}_i \mathbf{S}_j$$

LDA+U

Density-functional theory and strong interactions: Orbital ordering in Mott-Hubbard insulators

A. I. Liechtenstein

Max-Planck-Institut für Festkörperforschung, D-70506 Stuttgart, Germany

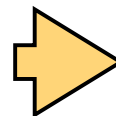
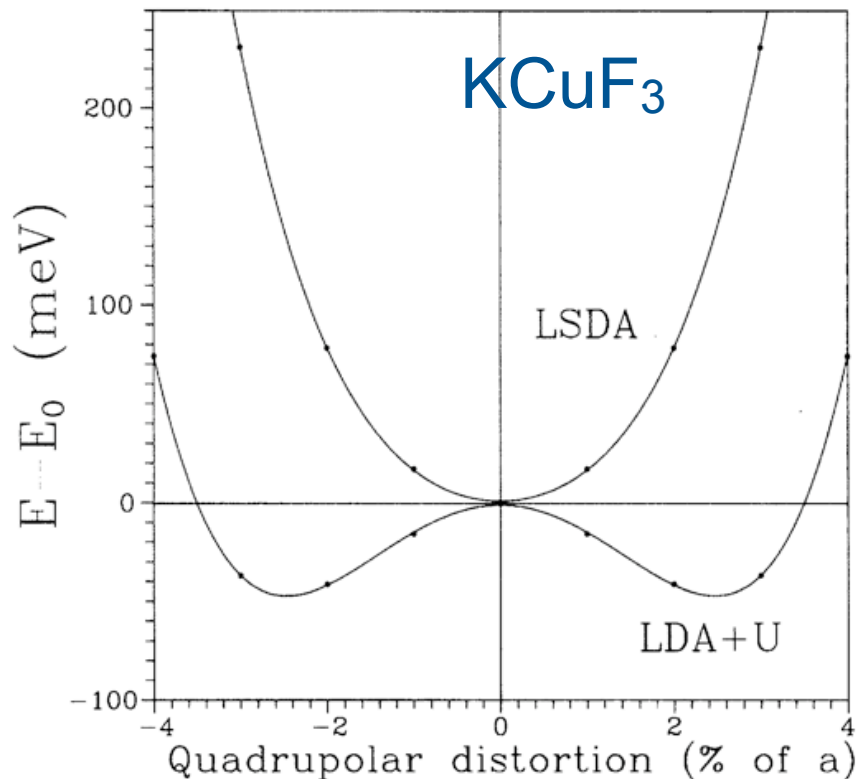
V. I. Anisimov

Institute of Metal Physics, GSP-170 Ekaterinburg, Russia

J. Zaanen

Lorentz Institute for the Theoretical Physics, Leiden University, Leiden, The Netherlands

(Received 15 May 1995)



The situation changes drastically if we allow for orbital polarization. Because U exceeds the bandwidth, the orbital sector is already strongly polarized (as are the spins) before the lattice is allowed to react. Overlooking some unimportant details concerning the coherence of the intermediate states, the well-known rule that electronic MFT in strong coupling maps onto the classical “spin” problem holds also in this case. In other words, we find the quadrupolar orbital-ferromagnetic spin phase to be most stable (for the same reasons as Kugel and Khomskii⁹). Obviously the cubic lattice is unstable in the presence of this orbital order parameter. In fact, despite large-scale changes in the electronic system the deformation is modest, indicating a rather weak electron-phonon coupling.

KK-like mechanism !

GGA+DMFT

PRL 101, 096405 (2008)

PHYSICAL REVIEW LETTERS

week ending
29 AUGUST 2008

Structural Relaxation due to Electronic Correlations in the Paramagnetic Insulator KCuF_3

I. Leonov,¹ N. Binggeli,^{1,2} Dm. Korotin,³ V.I. Anisimov,³ N. Stojić,^{4,2} and D. Vollhardt⁵

¹Abdus Salam International Center for Theoretical Physics, Trieste 34014, Italy

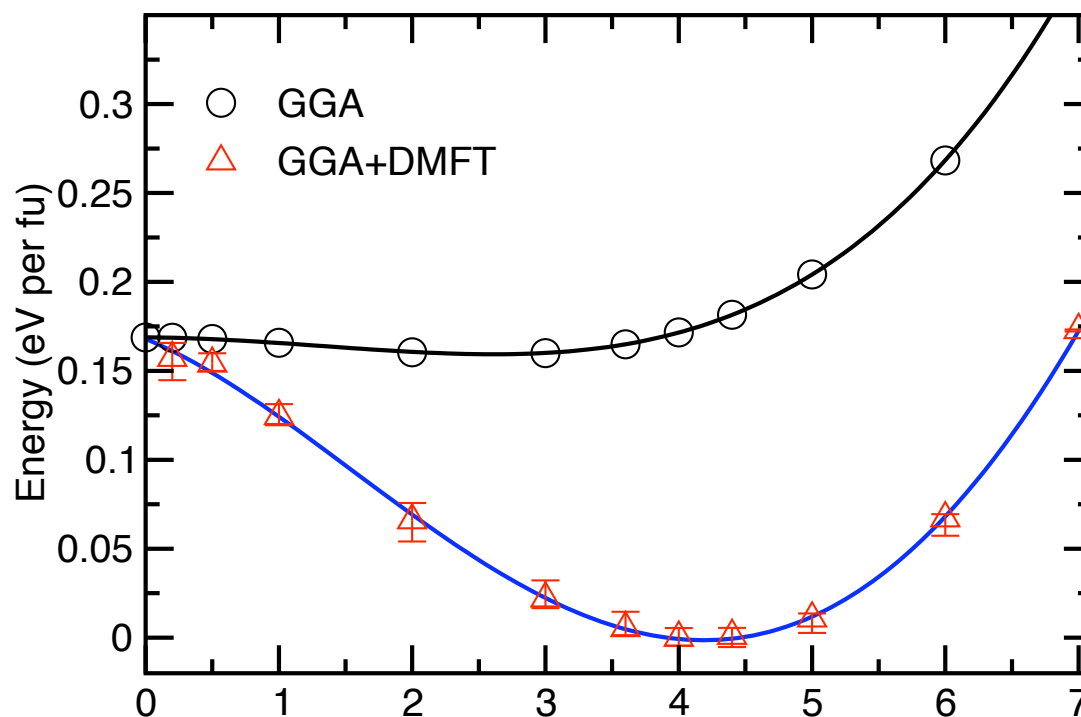
²INFM-CNR Democritos, Theory @ Elettra group, Trieste 34014, Italy

³Institute of Metal Physics, South Kovalevskoy Street 18, 620219 Yekaterinburg GSP-170, Russia

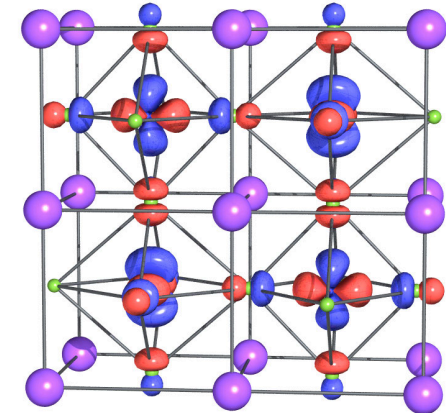
⁴International School for Advanced Studies, SISSA, Via Beirut 2/4, 34014 Trieste, Italy

⁵Theoretical Physics III, Center for Electronic Correlations and Magnetism, Institute of Physics, University of Augsburg, Augsburg 86135, Germany

(Received 7 April 2008; published 29 August 2008)



two scenarios



- super-exchange

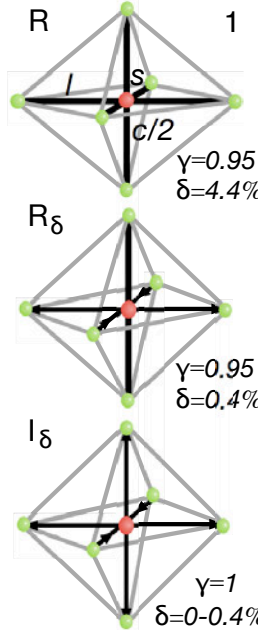
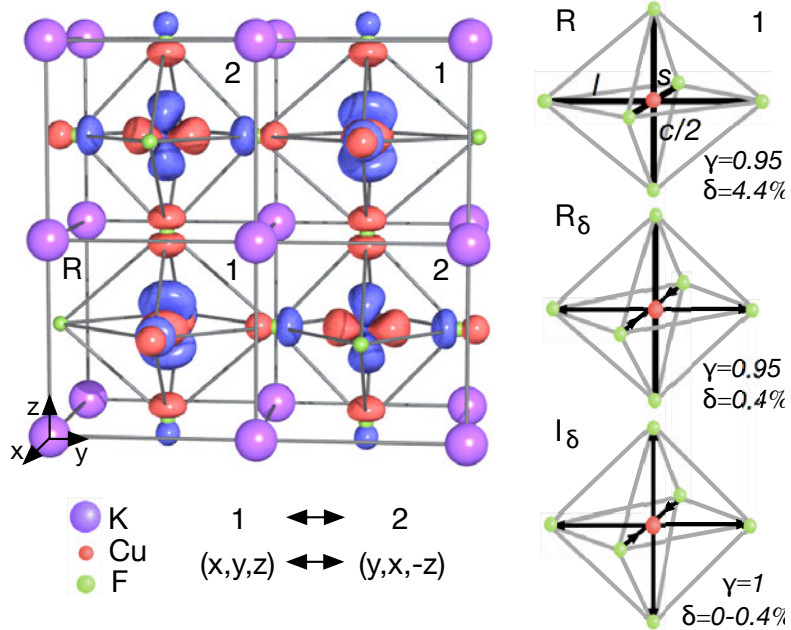
- why T_N (40K) much smaller than T_{OO} (800-1400 K) ?

- electron-phonon coupling

- what about LDA+U, HF, GGA+DMFT results?

Our approach: single out Kugel-Khomskii mechanism
using LDA+DMFT

KCuF₃

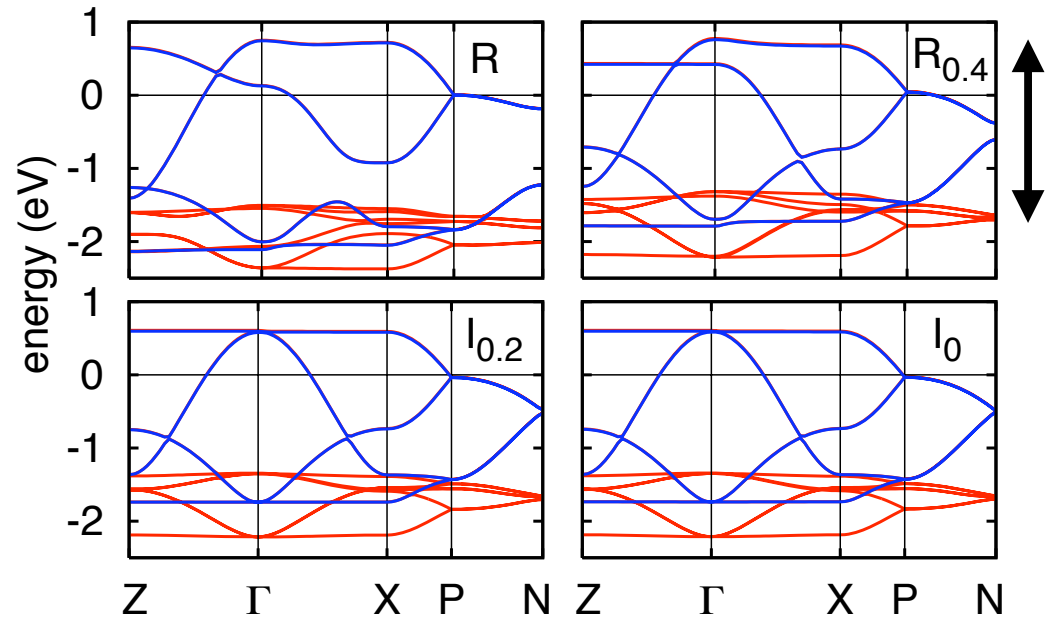


ideal structures

$\delta=(l-s)/(l+s)/2$ Jahn-Teller distortion

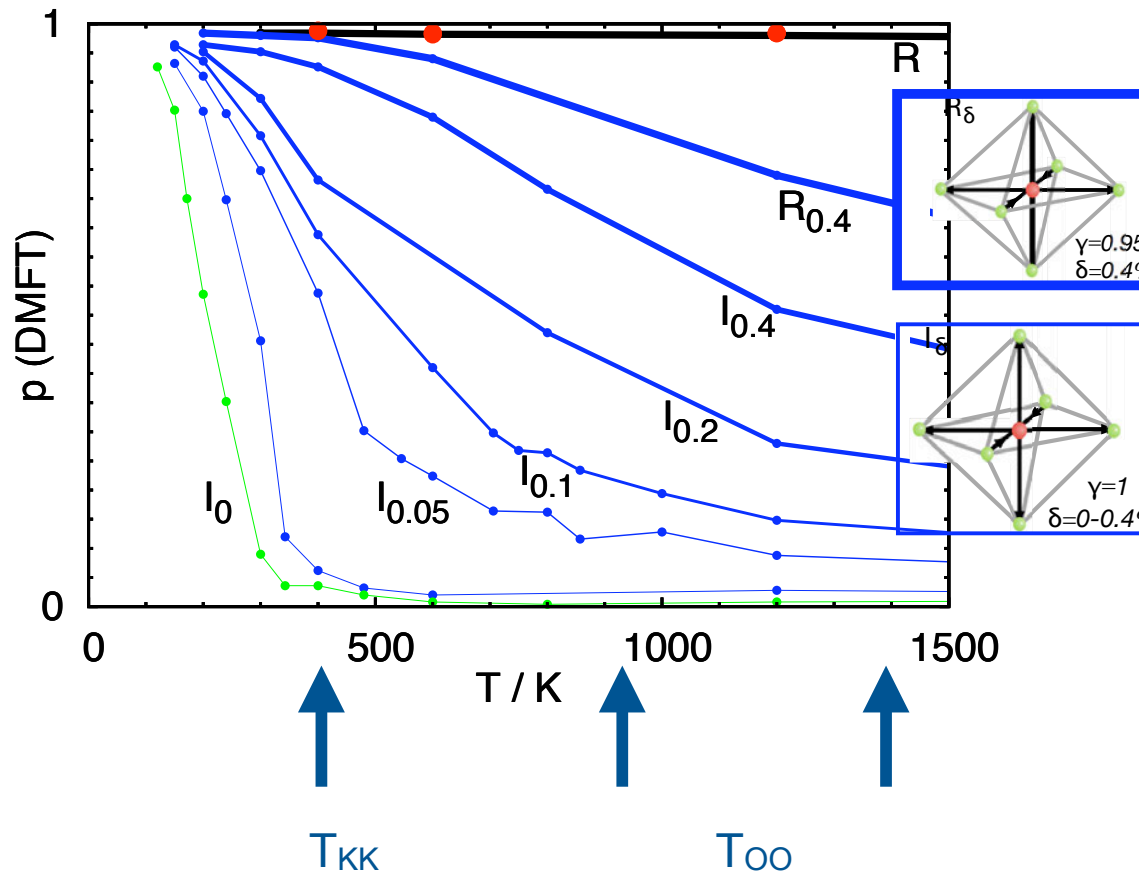
$\lambda=c/a/2$ tetragonal distortion

LDA bands
 NMTO-based downfolding method
 ab-initio model for e_g bands

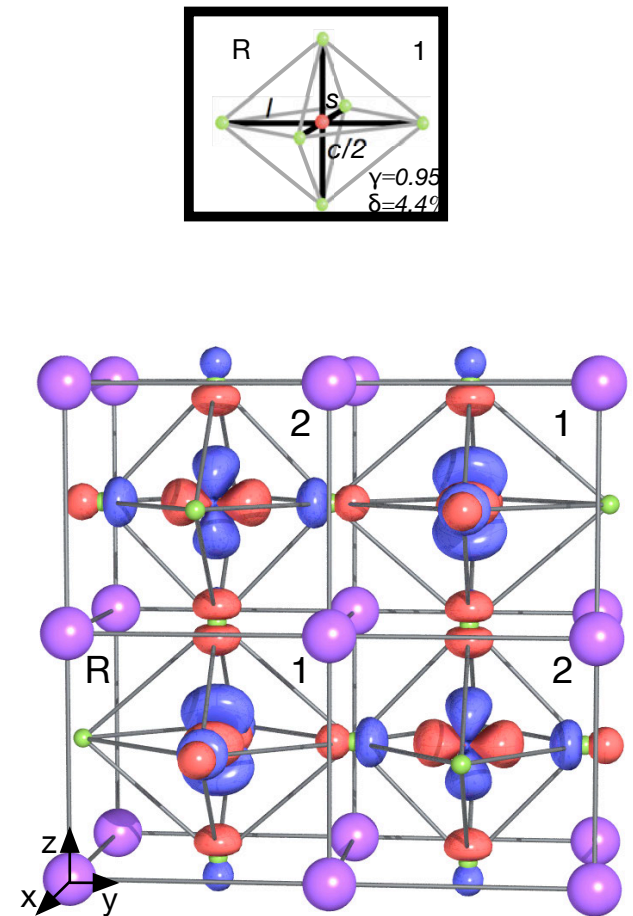


Mechanism for orbital ordering in KCuF_3

orbital polarization $p = n_1 - n_2$
for decreasing e-ph coupling g



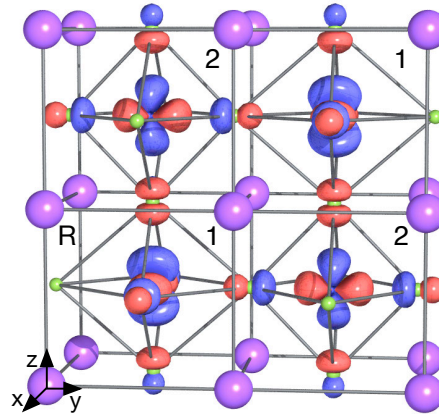
orbital ordering R structure



conclusions

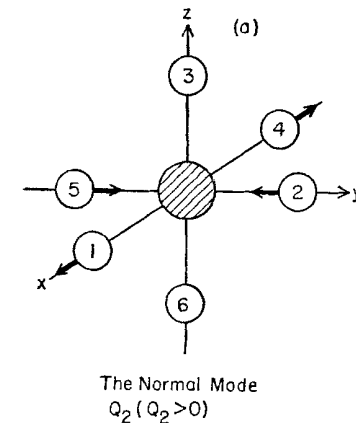
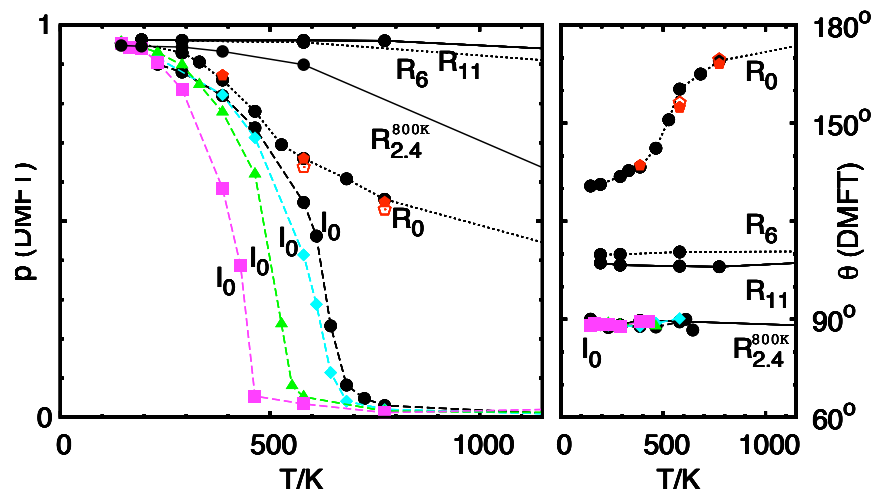
KCuF₃ and LaMnO₃

what is the mechanism of orbital-order?



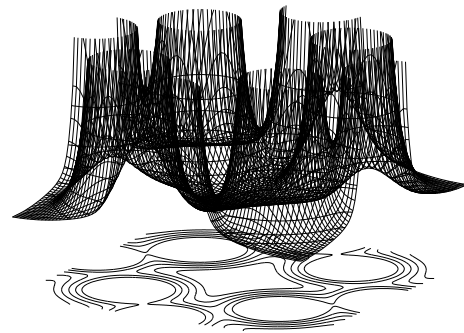
T_{KK} remarkably large

but el-ph coupling essential

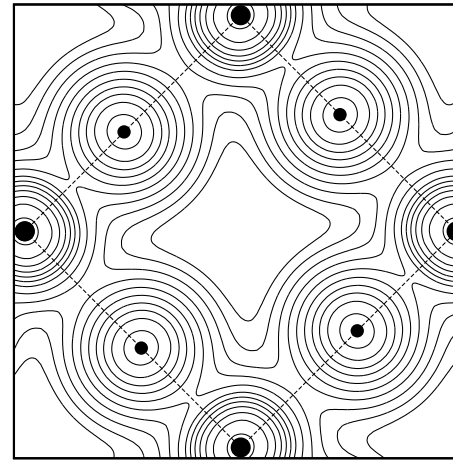


final remarks

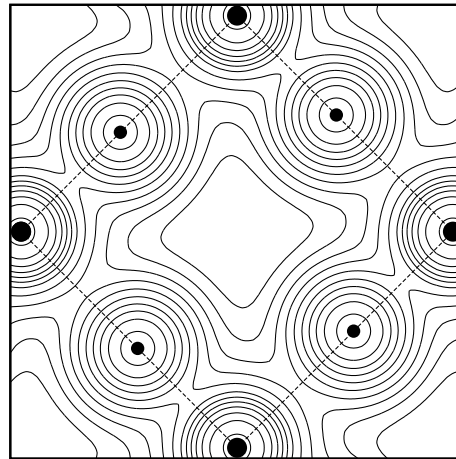
towards predictive power



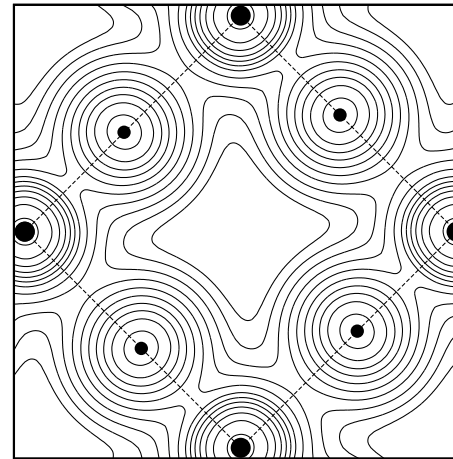
KCuF₃ (LDA+U)



KCuF₃ atomic



KCuF₃ (LSDA)



details matter...

towards predictive power

The effectiveness of this message may be indicated by the fact that I heard it quoted recently by a leader in the field of materials science, who urged the participants at a meeting dedicated to “fundamental problems in condensed matter physics” to accept that there were few or no such problems and that nothing was left but extensive science, which he seemed to equate with device engineering.

The main fallacy in this kind of thinking is that the reductionist hypothesis does not by any means imply a “constructionist” one: The ability to reduce everything to simple fundamental laws does not imply the ability to start from those laws and reconstruct the universe. In fact, the more the ele-

4 August 1972, Volume 177, Number 4047

emergent behavior



**Philp Warren
Anderson**

Nobel Prize in Physics 1977

SCIENCE

<http://www.emergentuniverse.org/>

identify which details do matters